공학박사학위논문

Anti-apoptotic Effect of *30Kc6* Gene on Induced Pluripotent Stem Cell, and Efficient Delivery of 30Kc19-based Transcription Factor Proteins for Cellular Direct Conversion

30Kc6 유전자를 이용한 역분화줄기세포의 세포자멸 억제 효과 및 세포의 직접변환을 위한 30Kc19 단백질 기반 전사인자의 효율적인 전달

2017년 8월

서울대학교 대학원

공과대학 협동과정 바이오엔지니어링

유 지 나

Abstract

Anti-apoptotic Effect of *30Kc6* Gene on Induced Pluripotent Stem Cell, and Efficient Delivery of 30Kc19-based Transcription Factor Proteins for Cellular Direct Conversion

Jina Ryu

Interdisciplinary Program for Bioengineering

The Graduate School

Seoul National University

30K protein, derived from silkworm hemolymph (SH), was known as having many properties. From 30K family (30Kc6, 30Kc12, 30Kc19, 30Kc21, and 30Kc23), 30Kc6 plays role for anti-apoptosis. When the cells were transfected with 30Kc6, the cells had higher viability in stress condition. Also, these property of 30Kc6 could increase the productivity of antibody, recombinant interferon-β, and human erythropoietin (EPO). The mechanism of 30Kc6 for anti-apoptosis was due to prevent Bax binding on mitochondria. The other 30K protein, 30Kc19, has reported the properties of cell-penetrating

and enzyme-stabilizing. Cell-penetrating peptide (Pep-c19) of 30Kc19 could enter cells by forming dimer. Also, 30Kc19 stabilized enzyme by crowd effect. Recent, 30Kc19 protein was reported enhancing soluble expression for transcription factors.

The objective of this research is to overcome several hurdles in stem cell research. Human pluripotent stem cells such as hESC and hiPSC suffer from apoptosis in single cell-dissociation. Because of pre-activated Bax at Golgi in cells, hESC and hiPSC induced rapid apoptosis in stress condition. We applied 30Kc6 in hiPSCs. hiPSC-30Kc6 was expressed pluripotent stem cell markers, and had a potency of differentiation in three germ layers. Also, the viability of single cells was higher than normal hiPSCs.

Then, we wondered that anti-apoptotic property of 30Kc6 was from a specific domain of 30Kc6. From the apoptosis research, BH4 domain of Bcl2 inhibited apoptosis by binding Bax. With structural similarity of BH4, 30Kc6 alpha-helix (30Kc6α) was considered as anti-apoptotic domain. By truncation, we cloned 30Kc6α and observed anti-apoptotic property. Furthermore, 30Kc19-30Kc6α protein could penetrate cell, and showed enhanced cellular viability under STS or UV-irradiation condition.

Cell-penetration and enzyme-stabilization are the properties on 30Kc19 protein. We tried to solve the problems on reprogramming which are instability and low solubility of transcription factor proteins. Previous reprogramming methods had a risk of transgene integration

to host genome. By using protein, transcription factors were delivered directly without any DNA-related complications. To express transcription factors as soluble form, 30Kc19 was conjugated. 30Kc19 conjugated transcription factors (Oct4, Sox2, c-Myc, and Klf4) were expressed as a soluble protein. Purified soluble transcription factors were penetrated into cells, and stable up to 48 h. Furthermore, Klf4-30Kc19 protein showed a transcriptional activity.

Lastly, we generated neuronal cells using transcription factor with 30Kc19. 30Kc19-Ascl1-NLS-R9 protein induced successfully mouse embryonic fibroblasts (MEFs) to protein-induced neuronal cells (p-iNCs). p-iNCs had neuronal morphology, and expressed neuronal markers (Tuj1 and MAP2). Furthermore, the expression levels of neuronal genes (*ASCL1, BRN2*, and *MYT1L*) were observed higher on day 7 and 14.

In this research, we applied anti-apoptotic 30Kc6 and cell-penetrating 30Kc19 protein on stem cell research. This approach will give a chance for developing new techniques in stem cell research.

Keywords: 30K protein, 30Kc6, 30Kc19, anti-apoptosis, cell penetration, recombinant protein, transcription factor, stem cell, direct conversion

Student Number: 2010-21054

Contents

List of Figures

List of Tables

List of Abbreviations

30Kc6 α : 30Kc6 alpha-helix

30Kc6 β : 30Kc6 beta-sheet

AP: alkaline phosphatase

ASC: adipose stromal cell

BF: bright field

BSA: bovine serum albumin

CCK-8: cell counting kit-8

CLSM: confocal laser scanning microscopy

CPP: cell-penetrating peptide

DAPI: 4',6-diamidino-2-phenylindole, dihydrochloride

DMEM: Dulbecco's modified Eagle's medium

E. coli: *Escherichia coli*

EB: embryoid body

EMT: epithelial-mesenchymal transition

ESC: embryonic stem cell

FACS: fluorescence-activated cell sorting

FBS: fetal bovine serum

FITC: fluorescein isothiocyanate

FPLC: fast protein liquid chromatography

GFP: green fluorescent protein

GOI: gene of interest

HDF: human dermal fibroblast

HeLa: Henrietta Lacks

HIV-1: human immunodeficiency virus-1

HRP: horseradish peroxidase

iPSC: induced pluripotent stem cell

IPTG: isopropyl 1-thio-β-D-galactopyranoside

MAP2: microtubule associated protein 2

MEF: mouse embryonic fibroblast

MSC: mesenchymal stem cell

MTT: 3,(4,5-dimethylthiazol-2-yl)2,3-diphenyltetrazolium

NLS: nuclear localization signal/ sequence

NS: non-significant

p-iNC: protein-induced neuronal cell

PS: penicillin-streptomycin

R9: nine-arginine

RT-PCR: real time-polymerase chain reaction

RT-qPCR: real time-quantitative polymerase chain reaction

SDS-PAGE: sodium dodecyl sulfate-polyacrylamide gel electrophoresis

SH: silkworm hemolymph

siRNA: short-interfering RNA

STS: Staurosporine

TALEN: transcription activator-like effector nuclease

TAT: trans-activator of transcription

Tuj1: neuron-specific class III beta-tubulin

Chapter 1.

Research background and objective

Chapter 1. Research background and objective

30K proteins are derived from silkworm hemolymph (SH), and introduced previously as a substitute for fetal bovine serum [1]. SH increased host cell longevity [2], and inhibited apoptosis in insect [3-5] and human cells [6]. Components of SH were isolated to identify the property [7, 8]. As a result, purified 30K proteins from SH had an interesting role for inhibiting apoptosis in various cells.

Among 30K protein family (30Kc6, 30Kc12, 30Kc19, 30Kc21, and 30Kc23), 30Kc6 had anti-apoptotic property in insect and mammalian cells [9]. 30Kc6 inhibited apoptosis with similar effect of whole SH. 30Kc6 protein was expressed in *Escherichia coli* (*E. coli*) [10], and the recombinant protein was tested anti-apoptotic effect by comparing with whole SH. Due to 30Kc6 protein was expressed in the form of an inclusion body, further denaturation and refolding steps were required. Although 30Kc6 has to be reconstructed, recombinant 30Kc6 protein also had effect of anti-apoptosis in insect (Sf9) and mammalian cell (HeLa) [11]. By using 30Kc6 anti-apoptotic property, the production rates of antibody [12], recombinant interferon-β [13], and human erythropoietin (EPO)

[14, 15] were increased.

The most abundant component, among 30K proteins, is 30Kc19 protein. 30Kc19 protein was reported cell-penetrating property in cells, also 30Kc19 protein could penetrate in *vivo* [16]. When 30Kc19 protein injected into mice, 30Kc19 protein was observed in various organ tissues. The mechanism for penetration was known as a dimerization by Cys-58 of 30Kc19 [17]. Cell-penetrating peptide (CPP) in 30Kc19 protein takes charge of these property. The cell-penetrating peptide of 30Kc19 protein (Pep-c19) was identified, and Pep-c19 was penetrated efficiently into cells, and delivered cargo proteins [18]. *In vivo* delivery, Pep-c19 dragged GFP in various organ tissues. Another property of 30Kc19 is enhancement stability of enzyme. By adding 30Kc19 protein with enzyme solution, the stability of alkaline phosphatase (AP) and horse radish peroxidase (HRP) was enhanced [19]. Furthermore, the stability of cellular mitochondrial enzyme complex and sialytransferase was increased by adding 30Kc19 protein to solution [20]. This stabilizing property is considered by non-specific crowding effect. Furthermore, 30Kc19 protein and human serum albumin nanoparticles were generated, and successfully delivered enzyme into cells or organs with low

cytotoxicity [21]. Recently, 30Kc19 N-terminal region (30Kc19α) was reported same or higher penetrating and stabilizing properties than 30Kc19 whole protein [22].

In this research, 30Kc6 anti-apoptotic protein and 30Kc19 cell-penetrating protein were applied to cellular engineering. First, 30Kc6 protein was used to cellular reprogramming to solve apoptosis derived from single cell-enzymatic dissociation. Then, to investigate the anti-apoptotic property of 30Kc6, we truncated 30Kc6 as N-terminal alpha helix region (30Kc6α). Then, 30Kc6α was conjugated with 30Kc19 protein in the purpose of cell-penetrating and soluble expression. By using multifunctional properties, 30Kc19 protein was also conjugated with reprogramming factors (Oct4, Sox2, c-Myc, and Klf4) for reprogramming. Lastly, 30Kc19-conjugated Ascl1 protein could induce mouse fibroblasts to neuronal cells.

In summary, the objectives of this study are:

1. Application of 30Kc6 anti-apoptotic protein on apoptosis derived from single cell-enzymatic dissociation in human induced pluripotent stem cell (hiPSC)

2. Investigation anti-apoptotic property of 30Kc6α, and protein expression of 30Kc6α with 30Kc19 cell-penetrating protein
3. Application of 30Kc19 cell-penetrating protein on production of reprogramming factors
4. Application of 30Kc19 cell-penetrating protein on direct conversion

In the thesis, 30Kc6 and 30Kc19 proteins were applied into cell engineering by using their properties. Especially, 30Kc6 could enhance viability of hiPSC. Also, 30Kc19 could help cellular reprogramming by conjugating with reprogramming factors. These findings may useful for study of regenerative medicine.

Chapter 2.

Literature review

Chapter 2. Literature review

2.1 Cellular reprogramming

Transcription factor is a protein that controls the gene regulation, and has the potential of being used as a drug. Since the finding of Yamanaka factors (Oct4, Sox2, Klf4, and c-Myc) [23, 24], research on cellular reprogramming has been actively carried out. This study offers unprecedented potential for disease research and regenerative medicine. Also, by generating induced pluripotent stem cells (iPSCs), the ethical problems from the use of embryonic stem cells (ESCs) can be avoided. Recent trend of cellular reprogramming is direct reprogramming, also known as transdifferentiation or direct conversion. Some transcription factors for direct conversion have been identified; such as MyoD for myoblasts [25], Gata4, Mef2c, and Tbx5 for cardiomyocytes [26], Ngn3, Pdx1, and Mafa for pancreatic beta cells [27], ETV2, FLI1, and ERG1 for endothelial cells [28], Ascl1, Brn2, and Myt1l for neurons [29], PDX-1 for insulin-producing cells [30]. Direct conversion is in the spotlight because it can be induced desired cells with high efficiency and short time.

Table 2.1 Examples for use of transcription factors in cellular reprogramming and direct conversion

Transcription factors	Cell type	References
Oct4, Sox2, Klf4, and c-Myc	iPSCs	[23,24]
MyoD	Myoblasts	[25]
Gata4, Mef2c, and Tbx5	Cardiomyocytes	[26]
Ngn3, Pdx1, and Mafa	Pancreatic beta cells	[27]
ETV2, FLI1, and ERG1	Endothelial cells	[28]
Ascl1, Brn2, and Myt1l	Neurons	[29]
PDX-1	Insulin-producing cells	[30]

2.2 Reprogramming methods

2.2.1 Virus

For reprogramming, the most conventional methods are viral transduction. Retrovirus generated iPSCs from various cell types for example mouse fibroblasts [23], human fibroblast [24, 31, 32], or human keratinocytes [33]. Retrovirus has 0.001−1% efficiency. Lentivirus is more efficient than retrovirus because it can infect both non−dividing and proliferating cells. The efficiency of lentivirus is 0.1−1.1%, and with high efficiency there are some reports for reprogramming using lentivirus [34−36]. Also, to control expression of transcription factors, inducible lentivirus is used. By using doxycycline−inducible lentiviral system, exogenous factors can be expressed when transactivator exists [37, 38] However, the use of retrovirus and lentivirus is limited due to the risk of tumorigenicity by incorporating of viral vector sequences into the host genome.

Non−integrating adenovirus or sendai virus can be alternative. Adenovirus transiently expressed transcription factors, and generated mouse and human iPSCs without genome−integration [39, 40]. Furthermore, hepatocytes transdifferentiated into insulin

producing cells by adenovirus-mediated gene transfer [30]. However, the efficiency of adenovirus was only 0.0001-0.001%. Sendai virus as non-integrating virus is an RNA virus, which does not enter the nucleus. By using sendai virus, iPSCs were generated from fibroblasts [41], cord blood cells [42], and T cells [43]. Although the efficiency of sendai virus is relatively high (0.1-1%), it required about 10 passages for losing viral gene, also the cells have to incubate at a higher temperature for removing temperature-sensitive virus.

2.2.2 DNA

To diminish the risk of integration, episomal plasmids, encoding transcription factors, were applied [44]. However, because transient expression is not maintained transcription factor for reprogramming, the reprogramming efficiency was low (0.0003-0.0006%) [34]. To overcome low efficiency, repeating transfection was tried. As a result, episomal plasmids could induced iPSCs. iPSCs by episomal plasmids were expressed pluripotent markers, and formed teratomas [45]. A nonviral minicircle plasmids had higher transfection efficiencies due

to lower activation of exogenous silencing mechanisms [46, 47]. Also, minicircle DNA vectors are free of bacterial DNA. Minicircle plasmids contained a cassette of transcription factors with a green fluorescent protein (GFP), and transfected cells were sorted by GFP [48]. There was a report about generation iPSCs from human adipose stromal cells (hASCs) by repeating transfection of minicircle DNA [49]. Exogenous plasmids were lost after 12 passages, and iPSCs were transgene-free condition. These DNA methods are advantageous in clinic because of the absence of genomic modification. However, the reprogramming efficiency is still low (~0.005%), and repeating transfection leads to cell damage [50].

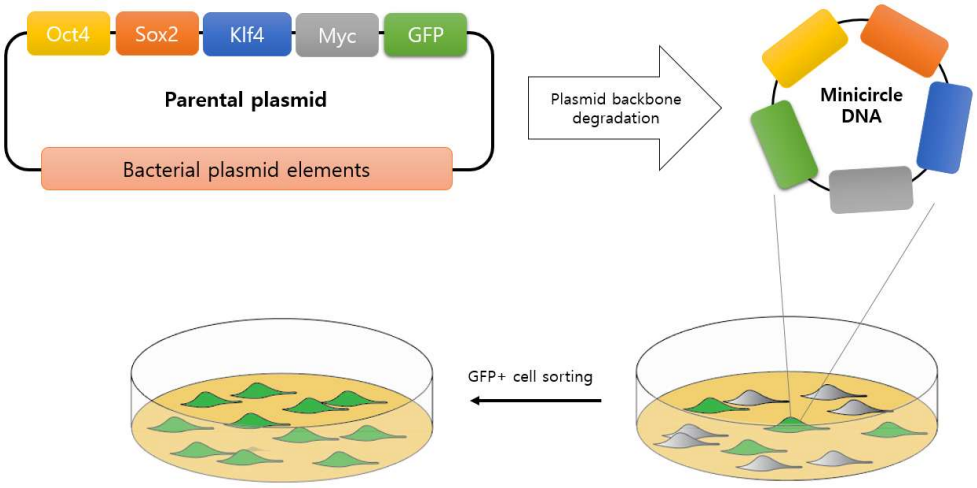

Figure 2.1 Minicircle DNA system and cell transfection

Parental plasmid includes reprogramming factors and GFP with bacterial plasmid elements. When arabionose is added, plasmid backbone is degraded, and minicircle DNA is remained. GFP is expressed in minicircle transfected cells. By FACS, GFP+ cells which are transfected reprogramming factors, are sorted.

2.2.3 mRNA and miRNA

RNA-induced pluripotent stem cells (RiPSCs) were successfully generated without genomic integration [51]. Also, using mRNA can generate footprint-free iPSCs. The efficiency of mRNA was reported 1.4% in human fibroblasts. From the study, RiPSCs were differentiated to myogenic cells. However, the methods are labor intensive and additional days are required for preparing mRNA. MicroRNA is another method for cellular reprogramming. There were studies of stromal cells and fibroblasts induced iPSCs using mir-200c plus mir-302s, and mir-369s family miRNAs [52]. Similarly, miR-302 and miR-372 induced human fibroblasts to iPSCs [53]. These miRNAs suppressed multiple downstream target genes, and controlled cellular process such as cell cycle and epithelial-mesenchymal transition (EMT). The cluster of the miR302/367 was reported for efficient method to generate iPSCs [54]. Due to the expression of miR302/367 activated Oct4 gene expression, miR302/367 iPSCs were showed similar characteristics to Oct4/Sox2/c-Myc/Klf4 iPSCs. The miRNA method takes shorter time than viral method. However, lower efficiency (~0.1%) has to solve.

2.2.4 *Cre/LoxP* and PiggyBac transposon

In the excision approach, *Cre/LoxP* recombination make iPSCs to be a factor-free condition. *Cre/LoxP* recombination is a more suitable for disease modeling. Somatic cells from Parkinson's disease patients were generated iPSCs, and differentiated successfully into dopaminergic neurons [55]. An excisable *loxP*-flanked lentiviral was also used for reprogramming [56]. The efficiency was reasonable (0.1 -1%), but *loxP* sites can retain in the genome.

Another excision approach is piggyBac transposon. Transposon is a footprint-free method because it is able to integrate into chromosome TTAA sites as a mobile genetic element, then transposon can excise in re-expression of the transposase [57]. Using piggyBac vector, human mesenchymal stem cells (MSCs) were generated to iPSCs with 0.02% efficiency [58]. The exogenous factors in iPSCs were removed completely. The hurdle of use for piggyBac transposon is that screening for excised lines is labor-intensive. Although the disadvantage, these excision methods are useful to apply regenerative medicine.

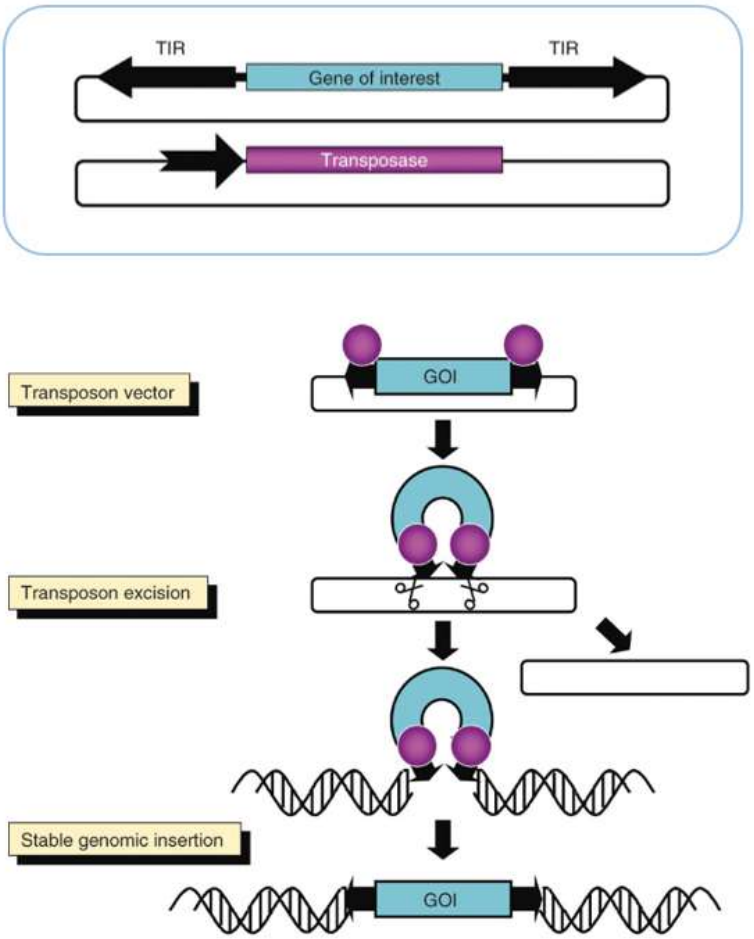

Figure 2.2 Transposon vector system

For transgene delivery, gene of interest (GOI) is between the transposon terminal inverted repeats (Black arrows). GOI is inserted into host plasmid by transposase (Pink spheres) [59].

2.2.5 Protein

Protein is considered as a safer method for cellular reprogramming due to direct delivery of transcription factors. There were not genomic integration and any of DNA-related complications. There were studies for reprogramming using direct delivery of proteins. Four reprogramming proteins (Oct4, Sox2, c-Myc, and Klf4) were produced in HEK cells [60]. By using these proteins, human fibroblast induced iPSCs with 0.001% efficiency. However, the concentration of delivered factors were limited due to cytotoxicity of the whole-protein extracts. To solve this problems, proteins were produced from *E. coli* expression system [61]. Four reprogramming proteins were produced in large scale from *E. coli*, and purified. Using these purified proteins, OG2/Oct4-GFP reporter MEF cells were induced iPSC, and expressed pluripotent markers. However, unlike mammalian proteins, *E. coli* proteins were formed aggregation and required extra refolding steps. Although the protein method is suitable to regenerative medicine with high safety, the limitations are short half-life of unstable protein. Also, large amount pure proteins are required for reprogramming.

Table 2.2 Methods for reprogramming and the efficiency

Methods		Efficiency (%)	References
Virus	Retrovirus	0.001−1	[32, 33]
	Lentivirus	0.1−1.1	[34−35, 38]
	Adenovirus	0.0001−0.001	[40]
	Sedai virus	0.1−1	[41−43]
DNA	Episomal plasmid	0.0003−0.0006	[44, 45]
	Minicircle DNA	−0.005	[50]
RNA	mRNA	1.4	[51]
	miRNA	−0.1	[54]
Cre/LoxP and Piggy Bac	*Cre/LoxP*	0.1−1	[56]
	PiggyBac	0.02	[58]
Protein	Protein	0.001	[60]

Chapter 3.

Experimental procedures

Chapter 3. Experimental procedures

3.1 Gene cloning

Template genes were obtained from Silkworm hemolymph total RNA (Kim et al. 2001) or Addgene (Oct4 #17217, Sox2 #17218, c-Myc #17220, Klf4 #17219, L-Myc #26022). The genes were amplified by reverse transcriptase polymerase chain reaction (RT-PCR). RT-PCR products were inserted into a pET23a vector (Novagen, Madison, WI, USA) for protein expression, and the vector was designed with a T7 tag at the N-terminus for immunoassay and His tag at the C-terminus for purification. For viral expression, RT-PCR products were inserted into a pMXs vector (Cell biolab, San Diego, CA, USA). The cloned genes were verified by GenoTech. (Daejeon, Korea). The restriction enzyme sites were used *Bam*H1, *Eco*R1, and *Xho*1.

3.2 Protein production and analysis

3.2.1 Protein expression and purification

Each vector was transformed to *E. coli* BL21 (Novagen), and cells

were cultured in LB medium with 100 μg/ml ampicillin. When OD600 reached 0.6 at 37℃, isopropyl-β-D-thiogalactopyranoside (IPTG) was added to a final concentration of 1 mM. For protein expression, the cells were further incubated at 27 or 37℃. Harvested cells were disrupted by ultra-sonication in a lysis buffer (20 mM Tris-HCl, 0.5 M NaCl, 20 mM imidazole, pH 8.0) and separated by centrifugation (12,000 rpm). The soluble proteins in the supernatant were collected and loaded on a HisTrap HP column (GE Healthcare, Uppsala, Sweden) using FPLC (GE Healthcare). The washing buffer (20 mM Tris-HCl, 0.5 M NaCl, 50 mM imidazole, pH 8.0) was placed into the column to remove unbound proteins. Finally, target proteins were eluted with the elution buffer (20 mM Tris-HCl, 0.5 M NaCl, 350 mM Imidazole, pH 8.0) and dialyzed against Tris-HCl (pH 8.0).

3.2.2 Quantitative analysis using BSA standard solution

For quantitative analysis of purified protein, the protein samples were analyzed by comparing with BSA standard solution. The proteins were mixed with 5 x sample buffer (0.25 M Tris-HCl, 0.5 M DTT, 10% SDS, 50% Glycerol, and 0.5% Bromphenol blue, pH 6.8),

then boiled for 5 min. The prepared protein samples and BSA standard solution were separated through 10% sodium dodecyl sulfate-polyacrylamide gel electrophoresis (SDS-PAGE), and stained by Coomassie Brilliant Blue (Thermofisher scientific, Waltham, MA, USA). After staining, the band size was calculated using Image J software. For high purity protein, Micro BCA™ Protein Assay Kit (Thermofisher scientitific) was used to analyze quantity of total protein.

3.2.3 Western blot analysis for *in vitro* stability assay

Purified soluble proteins were incubated in 37℃ for 24 or 48 h. After incubation, the samples were separated through 7.5% (protein size 70-120 kDa), 10% (30-70 kDa), and 12% (15-30 kDa) SDS-PAGE, and transferred onto a polyvinylidene difluoride (PVDF) membrane (GE Healthcare). The membranes were blocked with 5 % skim milk in TBS with 0.1% tween 20. Anti-T7 primary antibody (Abcam, Cambridge, UK) and anti-rabbit horseradish peroxidase (HRP)-conjugated secondary antibody (Millipore, Bedford, MA, USA) were used for immunoblot analysis. Luminata Forte Western HRP

Substrate (Millipore) was used as substrate of HRP. The band was visualized by G:BOX Chemi XL system (Syngene, Cambridge, UK), and the band intensities were quantified using Image J software.

3.3 Cell culture

3.3.1 Primary cell isolation and culture

For primary mouse embryonic fibroblast (MEF), 13.5 days pregnant mice (the C57/BL6 strain) were prepared. Embryos from the mice were harvested, then separated fibroblasts from embryos. The separated fibroblasts were washed twice with PBS, then dissociated as single cells using 0.25% trypsin-EDTA (Gibco, Carlsbad, CA, USA). After removal larger embryo fragments, the cells were incubated in 37℃ with MEF culture medium, Dulbecco's modified eagle medium (DMEM) with 10% fetal bovine serum (FBS, Gibco) and 1% penicillin streptomycin (PS, Thermofisher scientitific). Every 3-5 days later, the cells were transferred into new dish using trypsin-EDTA (Gibco).

3.3.2 Embryonic stem cell culture and embryoid body formation

Wild type of human embryonic stem cell (hESC), SNUhES31, and mouse embryonic stem cell (mESC) were offered from Institute of Reproductive Medicine and Population, Medical Research Center, Seoul National University, Seoul, Korea). Embryonic stem cells were cultured on feeder layers of mitomycin-C (Sigma-aldrich, St. Louis, MO, USA)-treated 2 x 10^5 STO cells per 35 mm gelatin-coated dish (ATCC® CRL-1503, Manassas, VA, USA) in DMEM/nutrient mixture F-12 ham (Thermofisher scientific) with 20% knockout serum replacement (Thermofisher scientific), 0.1 mM of 2-mercaptoethanol (Sigma-aldrich), 1% PS, 1% MEM non-essential amino acids solution (Thermofisher scientific), and 5 ng/ml of recombinant human FGF-2/FGF-basic (Biovision, Milpitas, CA, USA). Cells were passaged onto fresh STO cells every week by mechanical transfer. For feeder free, cells were cultured with essential 8 medium (Thermofisher scientific) on the geltrex® (Thermofisher scientific)-coated dish.

To form embryoid body (EB), hESCs were detached using

collagenase type Ⅳ (Gibco) 4 days after mechanical transfer. The detached colonies were suspended for 7 days on Petri dish (Thermofisher scientific). The medium was changed every 2-3 days in DMEM)/nutrient mixture F-12 ham (Thermofisher scientific) with 10% FBS (Gibco) and 1% PS (Thermofisher scientific). The EBs were harvested and the expression levels of pluripotency (*OCT4, NANOG*), ectoderm (*PAX6, ZIC1*), endoderm (*SOX17, GATA4*), and mesoderm (*GATA2, TAL1*) markers were analyzed by real-time quantitative PCR (RT-qPCR) on a StemOnePlus Real-Time PCR (Thermofisher scientific). The comparative C_T method ($\Delta\Delta C_T$) was calculated by normalization of *GAPDH*. The primer sequences are listed in Table 3.6.2.

3.4 Generation of induced pluripotent stem cell (iPSC)

3.4.1 Retrovirus production

Gp2-293 packaging cells (Clontech laboratories, Mountain view, CA, USA) were plated at 1 x 10^6 cells per 100 mm dish and incubated overnight. Cells were transfected with 30Kc6 and pVSV-G using Lipofectamine® 3000 (Invitrogen, Carlsbad, CA, USA) according to

the manufacturer's instructions. After 48 h incubation, the virus-containing medium was collected and filtered through a 0.45 μm membrane filter (Pall corporation, Washington, NY, USA). The virus was precipitated using Retro-ConcentinTM (System biosciences, Palo Alto, CA, USA). The precipitated virus was suspended using DMEM and stored at -70℃ for further use. DsRed containing virus was made for analysis of viral transduction efficiency.

3.4.2 Viral transduction and iPSC culture

Human dermal fibroblasts (ATCC® PCS-201-010) and isolated MEFs were seeded at 1 x 10^5 cells per 35 mm dish and incubated overnight. Oct4, Sox2, c-Myc, and Klf4 virus-containing DMEM medium was added to cells supplemented with 8 μg/ml of polybrene, and cells were incubated in 37℃ for more than 18 h. On the next day, the cells were incubated in new DMEM media and cultured for 3-5 days more. When colonies were appeared, the colonies were picked up using pasteur pipettes (Sigma-aldrich). The iPSC colonies were transferred on the new feeder every 5-7 days through the mechanical method.

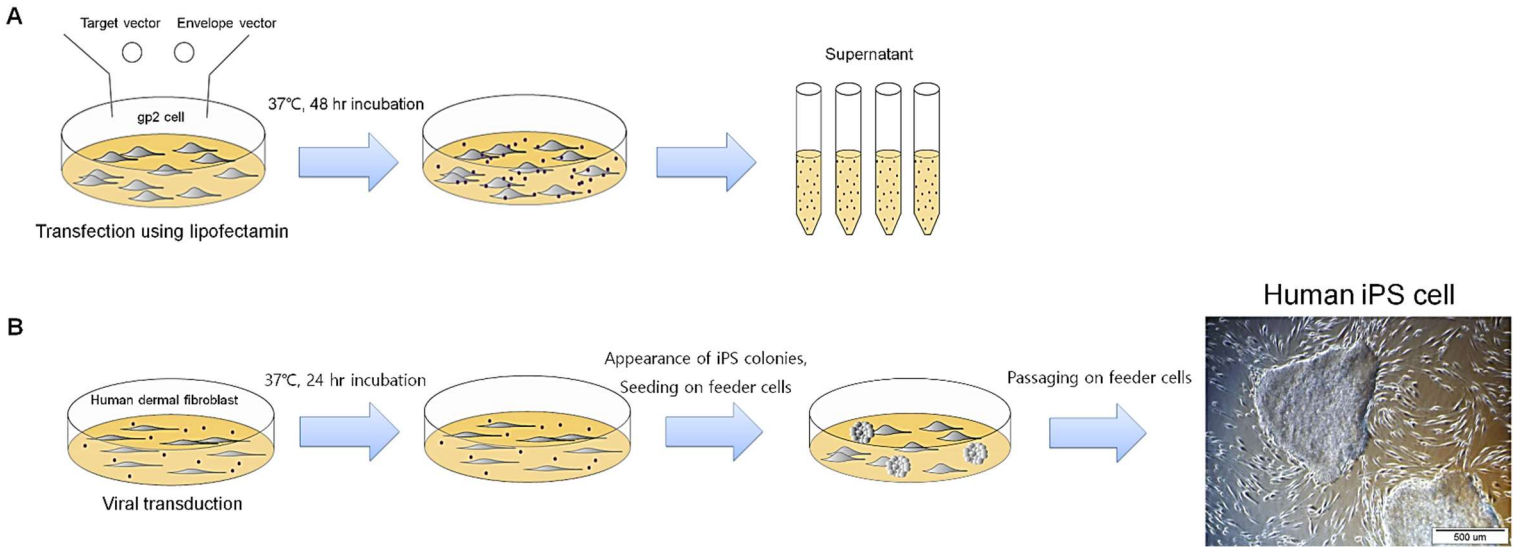

Figure 3.1 Procedure for generation of human iPSC

A. Retrovirus production. **B.** Viral transduction and iPSC culture.

3.5 Generation of protein-induced neuronal cell (p-iNC)

On day 0, isolated mouse embryonic cells (MEFs) and glial cells (astrocytes, obtained from Center for Medical Innovation, Seoul National University Hospital) were seeded and co-cultured in DMEM supplemented with 10% FBS and 1% PS. For the next 2 days, medium was exchanged with fresh media containing 30 μg/ml of reprogramming protein with 2 mM VPA (Thermo Fisher Scientific Inc.). On day 3, the medium was replaced with N3 media (DMEM/F12, N2 supplement, B27, 12.5 mg insulin, and PS) containing 30 μg/ml of reprogramming protein. On the next day, medium was replaced reprogramming protein-free N3 media. Proteins were treated every 3 days until day 14.

3.6 Cell analysis

3.6.1 RNA isolation and cDNA synthesis

hESCs and iPSCs were separated from feeder cells using collagenase type Ⅳ (Gibco, Carlsbad, CA, USA) and disrupted using 1 ml of TRI Reagent® (Sigma) per 5 x 10^6 cells. After addition of

200 μl of chloroform, cells centrifuged at 12,000 x g for 15 min at 4℃. An upper aqueous phase was collected and mixed isopropyl alcohol. After centrifugation at 12,000 x g for 10 min, the supernatant was removed and the pellet was washed with 75% ethanol. The synthesis of cDNA was using M-MLV cDNA synthesis kit (Enzynomics) according to manufacturer's instructions.

3.6.2 RT-PCR and quantitative RT-PCR

To amplify DNA, reverse transcription polymerase chain reaction (RT-PCR) was used. Template DNA and primers were added with AccuPower® PCR premix (Bioneer). For quantitative RT-PCR, 500 ng RNA was reverse transcribed into cDNA using the first Strand cDNA Synthesis kit (Promega) with SuperScript™ II reverse transcriptase. Template cDNA was amplified using SYBR Master Mix, and real-time quantitative PCR (RT-qPCR) was carried out on the Lightcycler® 480 System (Roche Applied Science). The comparative C_T method ($\Delta\Delta C_T$) was calculated by normalization of *GAPDH*. The primer sequences are listed in Table 3.6.2.

Table 3.6.2 Primers for real-time quantitative PCR

Gene		Sequence
OCT4	Forward	GAAGGATGTGGTCCGAGTGT
	Reverse	GTGAAGTGAGGGCTCCCATA
NANOG	Forward	TTCCTTCCTCCATGGATCTG
	Reverse	TCTGCTGGAGGCTGAGGTAT
PAX6	Forward	TTTGCCCGAGAAAGACTAGC
	Reverse	GGCCCTTCGATTAGAAAACC
ZIC1	Forward	AGCGACAAGCCCTATCTTTG
	Reverse	CGTGGACCTTCATGTGTTTG
SOX17	Forward	CATGACTCCGGTGTGAATCTC
	Reverse	CAGTAATATACCGCGGAGCTG
GATA4	Forward	AAAGAGGGGATCCAAACCAG
	Reverse	TTGCTGGAGTTGCTGGAAG
GATA2	Forward	ACCGGAAGATGTCCAACAAG
	Reverse	TCTCCTGCATGCACTTTGAC
TAL1	Forward	AAGTTGTGCGGCGTATCTTC
	Reverse	TCTTGCTGAGCTTCTTGTCC
ASCL1	Forward	AGGGATCCTACGACCCTCTTA
	Reverse	ACCAGTTGGTAAAGTCCAGCAG
BRN2	Forward	GACACGCCGACCTCAGAC
	Reverse	GATCCGCCTCTGCTTGAAT
MYT1L	Forward	CCTATGAGGACCAGTCTCCA

	Reverse	TCTTTTCTGTTCTTGAGGGATCTT
GAPDH	Forward	GTCAGTGGTGGACCTGACCT
	Reverse	TGCTGTAGCCAAATTCGTTG

3.6.3 Immunocytochemistry

For immunocytochemistry of cells, the cells were fixed using 4% paraformaldehyde (Sigma-aldrich) for 15 min, then permeabilized using 0.05% tween-20 (Amresco, Cleveland, OH, USA) for 2 h. Anti-Tra-1-60 (Abcam, Cambridge, UK) and anti-Oct4 (Santa Cruz Biotechnology, Dalls, TX, USA) were used as primary antibody (1:100). Anti-mouse Alexa 488-conjugated secondary antibody (1:250) was used for Tra-1-60, and Anti-rabbit Alexa 594-conjugated secondary antibody (1:250) was used for Oct4. Hoechst 33342 (Life Technologies, Gaithersburg, MD, USA) was stained on nucleus. The images were obtained by confocal fluorescence microscope (Olympus, Lake Success, NY, USA).

3.6.4 Live cell analysis

For live cell imaging, recombinant proteins were labeled with an Alexa Fluor® 488 protein labeling kit (Invitrogen). One M Solution of sodium bicarbonate was added to 1 ml deionized water. Then, 1 mg of target protein was mixed with the solution, and washed to remove unbound Alexa Fluor®. HDF cells were treated with labeled

proteins. Hoechst 33342 (Life Technologies, Gaithersburg, MD) was stained on nucleus and observed using confocal fluorescence microscope (Olympus).

3.6.5 Cell viability assay

To assess the toxicity of protein, HDF cells were treated with proteins in 96-well plate. Proteins were added into cells for 12 or 24 h. After treatment, cells were washed three times with PBS and treated with MTT solution for 4 h then solubilized for 12 h at 37℃. Absorbance at 420 nm was measured for the determination of cell viability. For use Cell Counting Kit-8 (Dojindo Laboratories, Kumanoto, Japan), the cells were incubated for 2 h with CCK-8 solution, and the absorbance at 450 nm was measured using a spectrophotometer.

3.6.6 Luciferase assay

pGL3-Klf4 reporter plasmid and pRL-SV40 (Addgene plasmid # 27163) were delivered into HEK293 cells using Lipofectamine®

3000 reagent (Invitrogen) according to the manufacturer's instructions. One day after the transfection, cells were treated with proteins. A Dual-Glo® luciferase assay system (Promega, Madison, WI, USA) was used for measurement of luciferase. On a 96-well plate (Nunc Lab-Tek, Thermo Scientific, Rockford, IL, USA), the cells were treated with proteins for 4 h and then washed with DMEM. Twenty microliters of a lysis reagent were added in 20 μl of DMEM medium. After 10 min of incubation, the firefly luminescence was measured using Luminometer (Thermo Scientific). Then 20 μl of stop reagent was added before measurement. The ratio of Firefly/Renilla luminescence was calculated, and each well was normalized from a control well.

3.6.7 Apoptosis induction and FACS analysis

For induction of apoptosis, hiPSC-30Kc6 and hiPSC were incubated with 0.5 μM of Staurosporine (Sigma-aldrich) and 20 mJ/cm^2. After additional 24 h incubation at 37℃, the cells were analyzed using flow cytometry. Before analysis, the cells were treated with Accutase^{TM} (Stem cell technologies, Vancouver, BC,

Canada) for single-cell dissociation after PBS washing twice. For flow cytometry analysis, the dissociated cells were washed and labeled with FITC Annexin V using FITC Annexin V Apoptosis Detection Kit (BD biosciences, San Jose, CA, USA). Cells ($1x10^6$) were collected and resuspended in 1 ml of 1x binding buffer. 100 μl ($1x10^5$ cells) of cell suspension was incubated with 5 μl of FITC Annexin V and 5 μl of propodium iodide (PI) for 15 min in dark room. Then 400 μl of 1x binding buffer was added. FACS Aria Ⅱ (BD biosciences) was used for analysis. The statistical analysis has been performed using SigmaPlot software. The p values were obtained from t-test in the software ($*p < 0.05$, $**p < 0.01$, $***p < 0.001$).

3.6.8 Single cell-dissociation and alkaline phosphatase staining

The colonies were dissociated to single cells using AccutaseTM, and 5 x 10^4 single cells were seeded on feeder. On day 7 of culture, the colonies were characterized by alkaline phosphatase staining. The AP positive colonies were counted using image J software. The statistical analysis has been performed using SigmaPlot software.

The p values were obtained from t-test in the software (*$p < 0.05$, **$p < 0.01$, ***$p < 0.001$). For alkaline phosphatase staining, the cells were washed twice with PBS after fixation, then stained using Leukocyte Alkaline Phosphatase Kit (Sigma-aldrich) according to the manufacturer's instructions. The stained cells were observed by optical microscope (Olympus).

3.6.9 Electrophysiological recording

The cells were observed on a submerged recording chamber (Warner instrument, Hadmen, CT, USA). A Multiclamp 700B amplifier (Molecular Devices, Foster City, CA, USA), Clampex 10.3 of the pClamp software package (Molecular Devices) were used for electrophysiological recordings. All recordings were patched using internal solution containing 115 mM potassium gluconate, 10 mM KCl, 10 mM HEPES, 10 mM EGTA, 5 mM Mg2+ -ATP and 0.5 mM 2Na+-GTP (pH7.3 and 280-285 mOsm). The extracellular solution contained 124 mM NaCl, 3 mM KCl, 1.3 mM MgSO4, 1.25 mM NaH2PO4, 26 mM $NaHCO_3$, 10 mM glucose and 2.4 mM $CaCl_2 \cdot 2H_2O$ (pH 7.3).

Chapter 4.

Anti-apoptotic effect of *30Kc6* gene on human induced pluripotent stem cell

Chapter 4. Anti-apoptotic effect of *30Kc6* gene on human induced pluripotent stem cell

4.1 Introduction

Since the finding of human induced pluripotent stem cell (hiPSC), several studies have been made on hiPSC. Attention has focused on the use of hiPSC in regenerative medicine by using their pluripotency. Also, hiPSC could avoid ethical issues that may arise in human embryonic stem cell. However, the culture of hiPSC is time consuming and labor intensive [62, 63]. Due to easily apoptosis in single cells, hiPSC is required to transfer as a form of colony (Figure 4.1).

There are several studies about genetic engineering of pluripotent stem cells to inhibit apoptosis. Penninger's group reported that inactivation of AIF renders had effect on inhibition of cell death in serum deprivation [64]. The suppression of p53 by short-interfering RNA (siRNA) enhanced the reprogramming efficiency by preventing apoptosis during culture [65]. Also, there was a report that over expression of Oct4 helps undifferentiated hESC survival under stress

[66]. By using nuclease, transcription activator-like effector nucleases (TALENs) was engineered genetically in hESC and hiPSC [67].

In this study, we applied 30Kc6 anti-apoptotic gene to hiPSCs. We hypothesized that 30Kc6 could inhibit apoptosis in hiPSC as like inhibiting apoptosis in other mammalian cells [9, 12, 68].

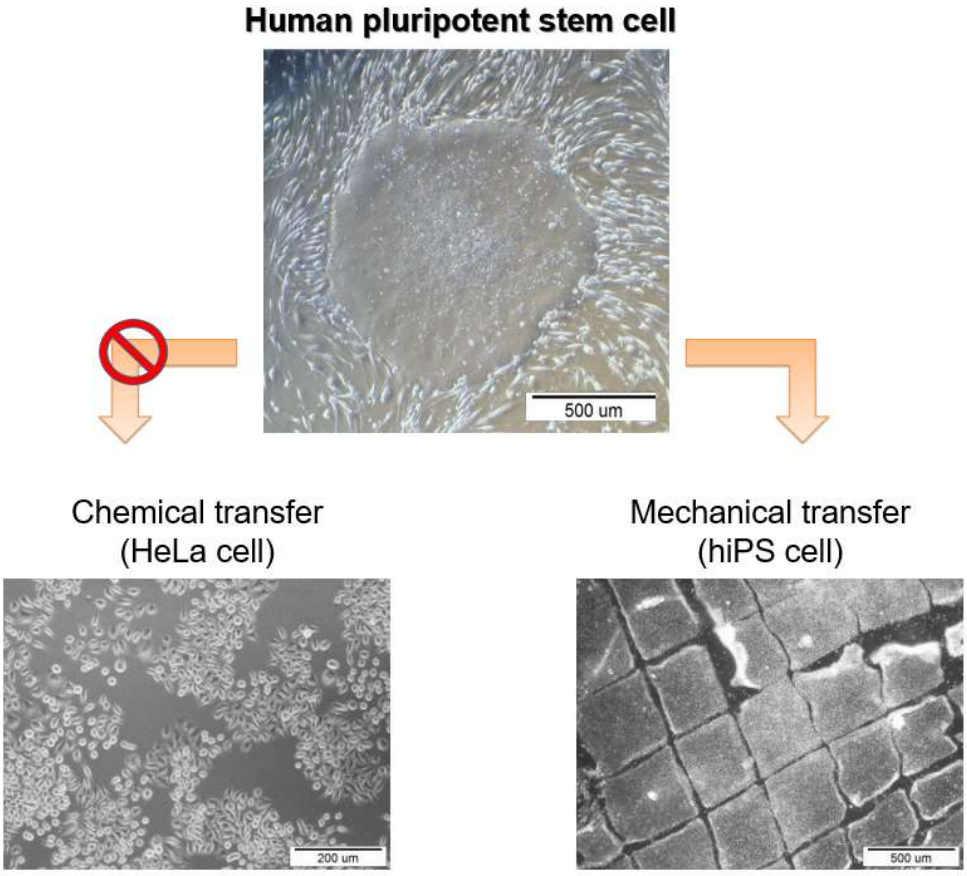

Figure 4.1 Human pluripotent stem cell (hPSC) colony in culture, and mechanical transfer

4.2 Retroviral transduction and expression of hESC-specific genes in hiPSC-30Kc6

OCT4, SOX2, c-MYC, KLF4, 30Kc6, or DsRed retrovirus were produced respectively. By using DsRed, a transduction efficiency of retrovirus on HDF cells was tested, and many of DsRed-fluorescent cells were observed in virus-treated HDF cells (Figure 4.2 A). Like fluorescent image, the results of flow cytometry were showed that the transduction efficiency was 73.6%. With high transduction efficiency, viral OCT4, SOX2, c-MYC, and KLF4 were treated on HDF cells for reprogramming. At the same time, we also added viral 30Kc6 in order to generate hiPSC-30Kc6. Therefore, hiPSC and hiPSC-30Kc6 were generated from HDF cells. To observe the expression of human embryonic stem cell (hESC)-specific genes in hiPSC-30Kc6, the cells were lysed, and cDNA was synthesized from mRNA. From Figure 4.2 B, RT-PCR results showed that hiPSC-30Kc6 expressed 30Kc6 gene as well as hESC-specific genes, including OCT4, SOX2, c-MYC, KLF4, and NANOG. Thus, we established hiPSC line containing with 30Kc6, and it expressed hESC-specific genes as like hiPSC and hESC.

hiPSC-30Kc6 has been cultured stably for more than 15 passages

on the feeder cells, and we observed the tightly compact colonies. The morphology of hiPSC-30Kc6 was round, and the colonies had clearly defined edges (Figure 4.2 C). Due to essential process to check whether pluripotent properties were existing or not after exogenous gene insertion, pluripotency markers (Tra-1-60 and Oct4) were analyzed by immunocytochemistry. From fluorescence image, hiPSC-30Kc6 expressed well Tra-1-60 and Oct4 as like hiPSC, and hESC. Although the nuclei were stained in all cells including feeder cells, Tra-1-60 and Oct4 were stained only in pluripotent stem cells. Moreover, alkaline phosphatase (AP) activity, an undifferentiated marker, was observed by staining (Figure 4.2 D). We observed that the colonies of hiPSC-30Kc6 were stained with strong AP activity. From these results, we concluded that hiPSC-30Kc6 was generated without loss of pluripotency.

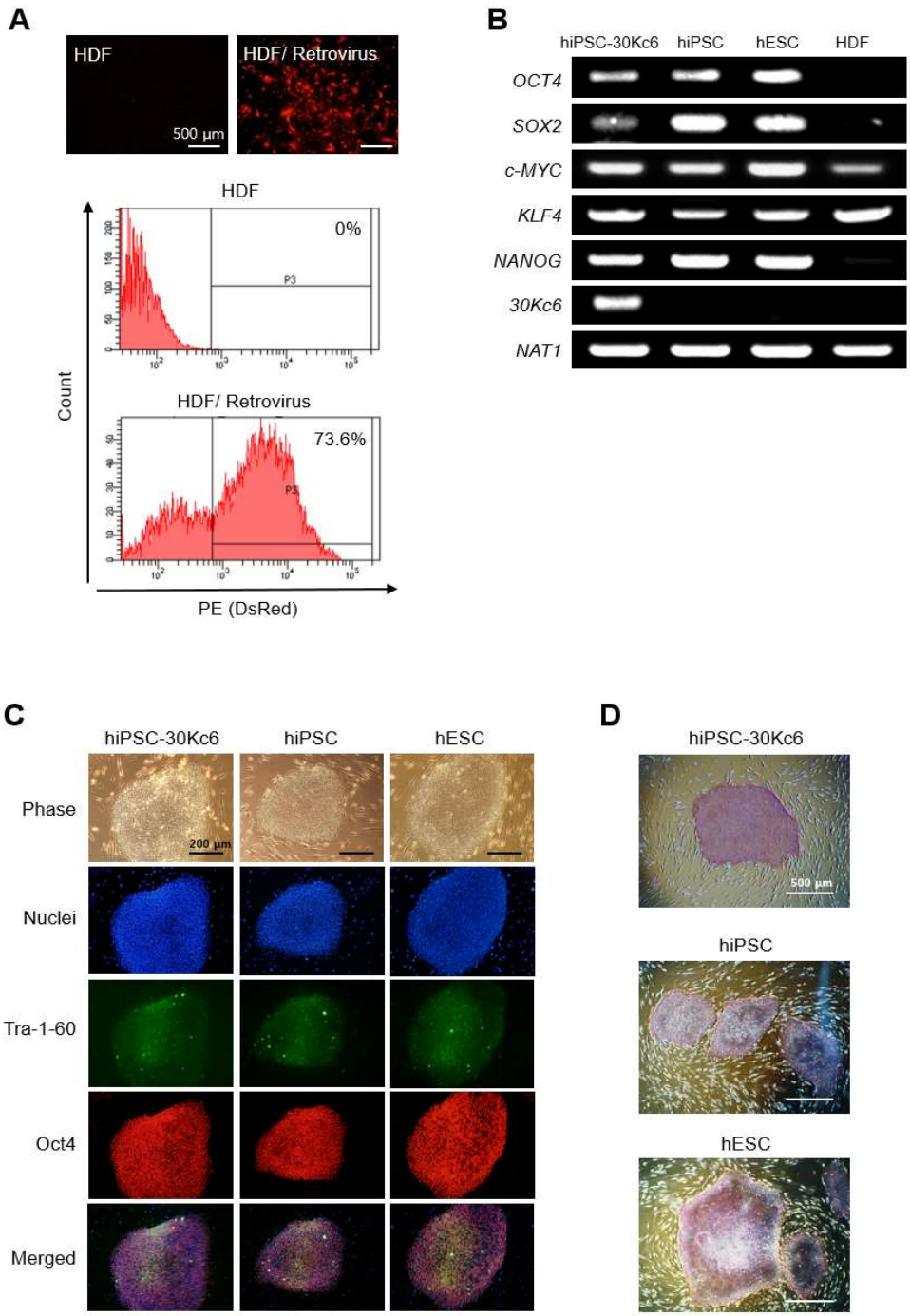
A
HDF
HDF/ Retrovirus
500 μm
HDF
0%
P3
Count
HDF/ Retrovirus
73.6%
P3
PE (DsRed)
B
hiPSC-30Kc6
hiPSC
hESC
HDF
OCT4
SOX2
c-MYC
KLF4
NANOG
30Kc6
NAT1
C
hiPSC-30Kc6
hiPSC
hESC
Phase
200 μm
Nuclei
Tra-1-60
Oct4
Merged
D
hiPSC-30Kc6
500 μm
hiPSC
hESC

Figure 4.2 Retroviral transduction on HDF cells and expression of pluripotent markers

A. FACS analysis for the efficiency of viral transduction (DsRed). **B.** RT-PCR analysis of endogenous hESC-specific genes and *30Kc6* gene in hiPSC-30Kc6. **C.** Immunocytochemistry of pluripotency markers, Tra-1-60 (Green) and Oct4 (Red). Nuclei were stained by Hoechst 33342 (Blue). Scale bar, 200 μm. **D.** Alkaline phosphatase staining. Scale bar, 500 μm.

4.3 *In vitro* differentiation of hiPSC-30Kc6

To check differentiation potency of hiPSC-30Kc6, we generated embryoid body (EB). On day 7 after formation, the size of EB was about 300 μm diameter (Figure 4.3 A). Then, EBs were collected and analyzed specific markers by RT-qPCR. On figure 4.3 B, hiPSC-30Kc6 was showed that pluripotency markers (*Oct4, Nanog*) were decreased, although the differentiated markers, ectoderm (*PAX6, ZIC1*), endoderm (*SOX17, GATA4*), and mesoderm (*GATA2, TAL1*), were increased. The values from RT-qPCR were normalized to GAPDH. It was similar results with hESC and hiPSC. This data indicated that hiPSC-30Kc6 had potency of differentiation in three germ layer. Therefore, we had no doubt that the insertion of 30Kc6 in hiPSC did not affect to differentiation potency.

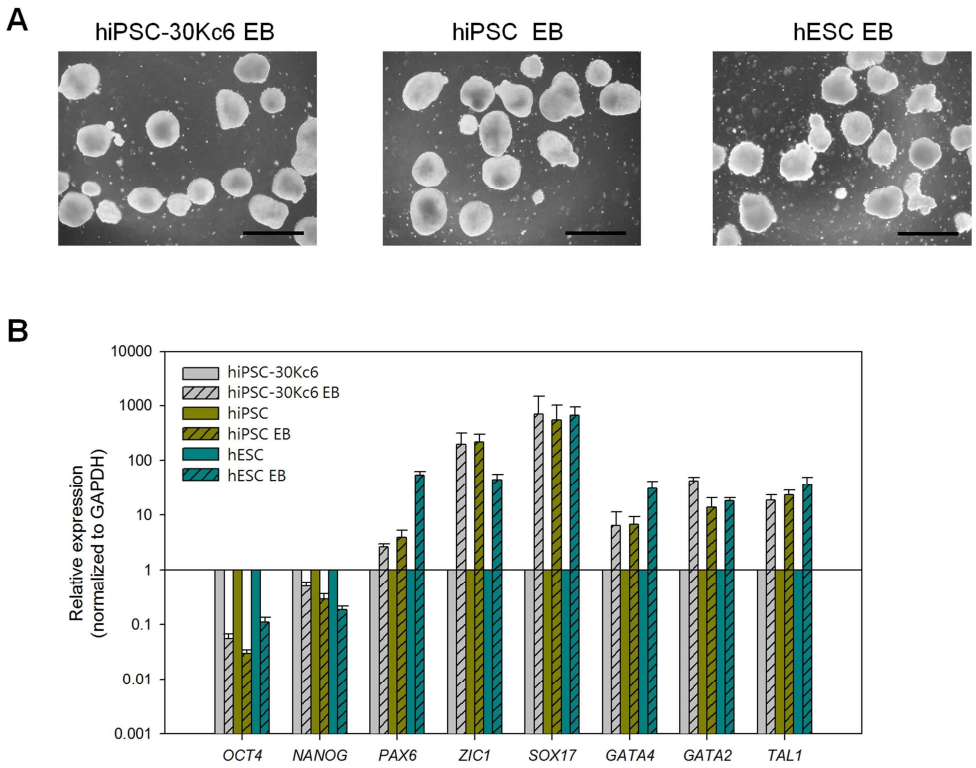

Figure 4.3 *In vitro* differentiation of iPSC-30Kc6

A. Embryoid body (EB) formation at day 7. Scale bar, 500 μm. **B.** Real-time quantitative PCR analysis of differentiated EB. Pluripotency (*OCT4, NANOG*), ectoderm (*PAX6, ZIC1*), endoderm (*SOX17, GATA4*), mesoderm (*GATA2, TAL1*) markers. Error bars represent standard deviation (n=3).

4.4 Anti-apoptosis effect on hiPSC-30Kc6

In previous study, we observed that 30Kc6 inhibit apoptosis in insect and mammalian cells [9, 12, 68]. 30Kc6 prevented the binding of Bax to mitochondria, therefore cytochrome c was not released [12]. We hypothesized that 30Kc6 could inhibited apoptosis on hiPSCs. To induce apoptosis, we treated 0.5 μM of Staurosporine (STS) to cells. The apoptotic cells were detected by Annexin V, then analyzed by flow cytometry (Figure 4.4). Two colonies of hiPSC-30Kc6 or hiPSCs were selected randomly, and analyzed. After 4 h of STS treatment, the percentage of Annexin V positive cells in hiPSC-30Kc6 were relatively lower than hiPSCs (Figure 4.4 A). hiPSC-30Kc6 #1 and hiPSC #1 which were the lowest apoptotic cells, were selected, and further experiments were processed. After 24 h treatment of STS, there were considerable difference between hiPSC-30Kc6 and hiPSC (Figure 4.4 B). hiPSCs showed 14.2% apoptosis. It was 1.43 times higher than the percentage of apoptosis in STS treated hiPSC-30Kc6, which was 9.9%. Another apoptosis was induced by UV-irradiation (Figure 4.4 C). Because UV-irradiation induced both intrinsic and extrinsic apoptosis, apoptotic cells were analyzed by caspase-3 activity. Relative caspase-3

activity of hiPSC was 1.42 times higher than that of hiPSC-30Kc6. From the result, we confirmed that 30Kc6 anti-apoptotic property is also working on hiPSC.

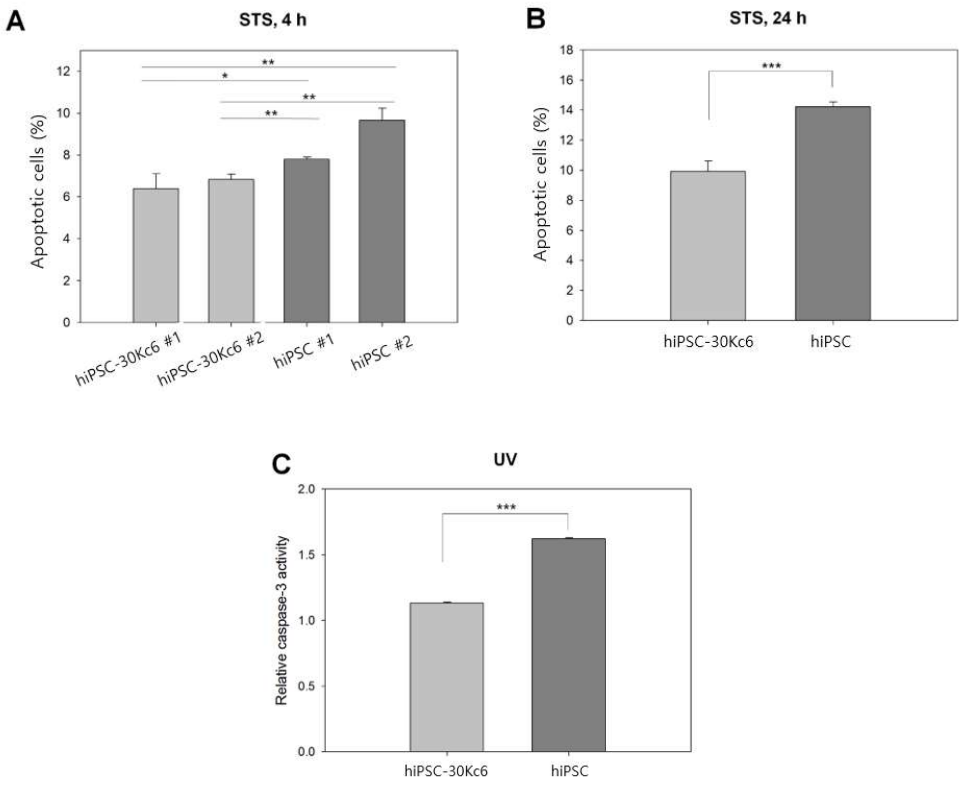

Figure 4.4 Anti-apoptotic property in hiPSC-30Kc6

A. FACS analysis for Annexin V positive apoptotic cells after 4 h of STS treatment. **B.** 24 h of STS treatment. **C.** Casepase-3 activity assay after 20 mJ/cm^2 UV-irradiation. $*p < 0.05$, $**p < 0.01$, $***p < 0.001$ compared with the control group (n = 3). Error bars represent standard deviation.

4.5 Single cell-dissociated cell viability

Due to single cells of hiPSC are weak to apoptosis, the subculture of colonies is required. We have tried to apply 30Kc6 on single cell-dissociation. Before single cell-dissociation, hiPSC-30Kc6 and hiPSC were cultured on feeder free condition. Cells were dissociated by Accutase^{TM}, then 5 x 10^4 cells were seeded on the feeder (Figure 4.5 A). On day 7 after seeding, the most colonies were grown up about 200 μm diameter. AP staining was performed, and AP positive colonies were analyzed by image J software (Figure 4.5 B). With identification of the size (fixel) and circularity of colonies, non-specific stain or the colonies which were derived from non-single cells were excluded for counting. Figure 4.5 C showed that the number of AP positive colonies in hiPSC-30Kc6 was on the average approximately 21, and it is 3 times higher than the number of AP positive colonies in hiPSC (approximately 7). This results indicated that single cell-dissociated cell viability was enhanced by 30Kc6 on hiPSCs.

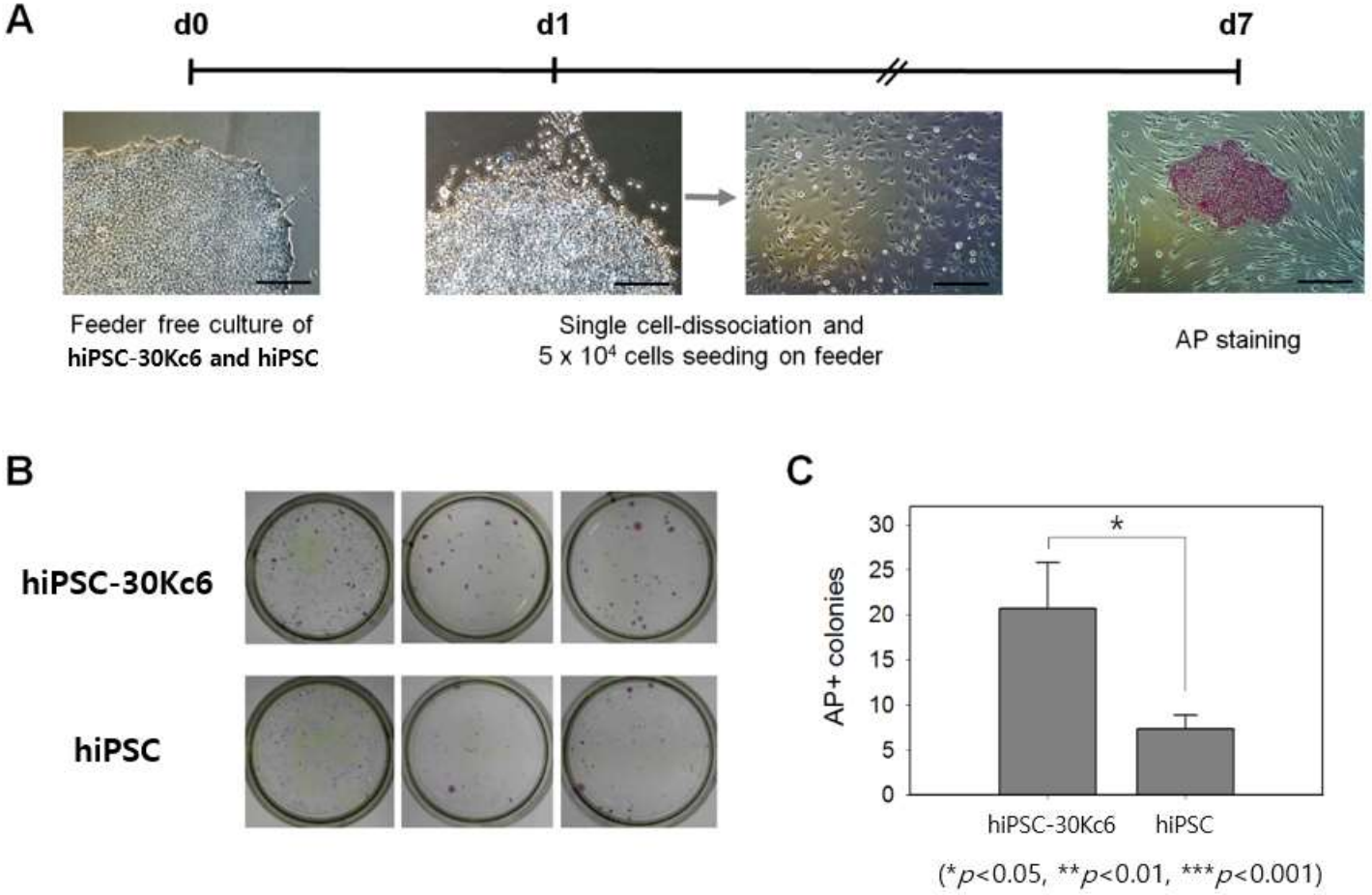
A
d0
d1
d7
Feeder free culture of
hiPSC-30Kc6 and hiPSC
Single cell-dissociation and
5 x 10⁴ cells seeding on feeder
AP staining
B
hiPSC-30Kc6
hiPSC
C
AP+ colonies
30
25
20
15
10
5
0
*
hiPSC-30Kc6
hiPSC
(*p<0.05, **p<0.01, ***p<0.001)

Figure 4.5 Cell viability on single cell-enzymatic dissociation

A. Procedure of cell-dissociation using Accutase™. Feeder free culture of hiPSC-30Kc6 and hiPSC at day 0. Single cell-dissociation and 5 x 10^4 cells were seeded on feeder at day 1. At day 7 alkaline phosphatase (AP) staining was performed.
B. AP staining dishes. C. The number of AP+ colonies counting by image J software. $*p < 0.05$ (n = 3). Error bars represent standard deviation.

4.6 Conclusions

To overcome the problems for easily induced apoptosis in hiPSCs, we introduced 30Kc6 anti-apoptotic gene in hiPSCs. First, hiPSC was transformed by expressing 30Kc6 protein. After several passaging, we confirmed the hiPSC-30Kc6 stable cell expressed pluripotency markers (Oct4, Tra-1-60, and alkaline phosphate). When the cells were induced apoptosis by Staurosporine, hiPSC-30Kc6 cell was showed the 1.4 times less Annexin V expression comparing with normal hESC or hiPSC. Moreover, the viability of enzymatic single cell dissociation was 3 times increased in hiPSC-30Kc6 by comparing with normal hiPSC. It means that the introduction of 30Kc6 seems to affect hiPSC by inhibiting of apoptosis. Therefore, the technology using 30Kc6 is anticipate to be used on stem cell engineering.

Chapter 5.

Anti-apoptotic role of 30Kc6 alpha helix domain and its application by conjugating with 30Kc19 protein

Chapter 5. Anti-apoptotic role of 30Kc6 alpha helix domain and its application by conjugating with 30Kc19 protein

5.1 Introduction

Apoptosis is known as programmed cell death, which is related to many diseases such as Alzheimer's disease and Parkinson's disease [69, 70]. Study of the inhibition of apoptosis is a required field not only for the treatment of these diseases, but also for the production of valuable products in biotechnological industry.

Previously in our study, 30Kc6 from Silkworm hemolymph has shown anti-apoptotic effect in preventing Bax translocation [12]. But the effect was not consistent and the mechanism was not clear. In this study, for more understanding of 30Kc6 anti-apoptosis property. 30Kc6 was truncated into N-terminal all-alpha (30Kc6α) and C-terminal all-beta (30Kc6β) domains by SWISS-MODEL program-based sequences. Anti-apoptotic Bcl2-family proteins such as Bcl-2, Bcl-XL, and Mcl-1 have a general structure that consists of a α-helix [71]. BHRF1, Epstein-Barr virus-encoded protein, was

reported anti-apoptotic property [72]. The interaction of BHRF1 with Bim BH3 domain inhibit the activity of pro-apoptotic Bim protein (Figure 5.1 A). We hypothesized that 30Kc6α could have potential to interact with pro-apoptotic proteins with structural basis (Figure 5.1 B). Thus, we truncated 30Kc6α from 30Kc6, and tested the anti-apoptotic property. Then, to express protein, 30Kc6α was conjugated with 30Kc19 cell-penetrating protein. 30Kc19-30Kc6α recombinant protein had cell-penetrating and anti-apoptotic properties. This recombinant protein is anticipated in use to clinic for apoptosis-related disease.

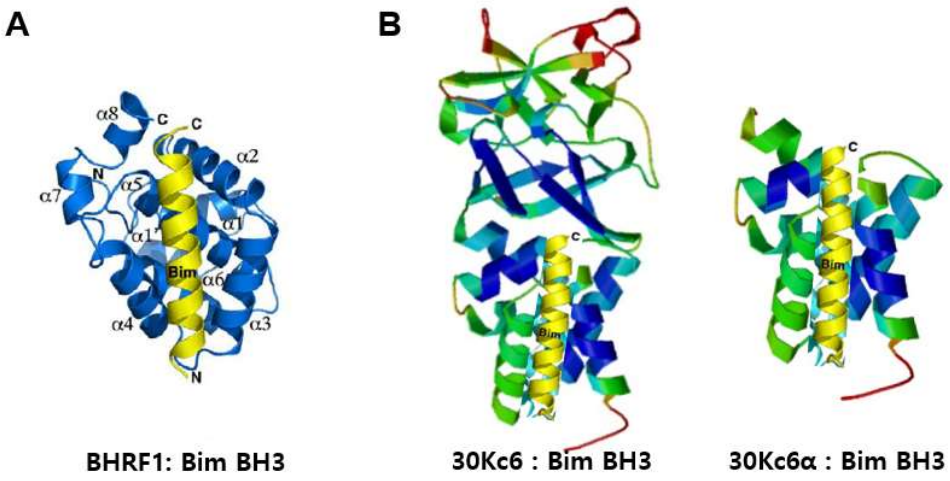

Figure 5.1 Apoptosis inhibition by structural basis

A. The interaction of BHRF1 protein with Bim BH3 [72]. B. The expected interaction of 30Kc6 or 30Kc6 α with Bim BH3.

5.2 Cloning of 30Kc6α and gene expression in mammalian cells

30Kc6 protein had two distinct regions; N-terminal all-alpha (30Kc6α) and C-terminal all-beta (30Kc6β) domains. By SWISS-MODEL program, 30Kc6 was truncated two separate proteins (Figure 5.2 A). 30Kc6α included amino acids 1-88, and 30Kc6β was amino acids 89-237 of 30Kc6 (Figure 5.2 B). With structural basis of 30Kc6α, we tested 30Kc6α to observe anti-apoptosis by comparing with 30Kc6. Fist, 30Kc6α were cloned in pcDNA3.1 vector. When the cells were transfected to 30Kc6α, the proteins were expressed in cells (Figure 5.2 C). Therefore, we observed that new designed 30Kc6α could express in cells with proper protein size.

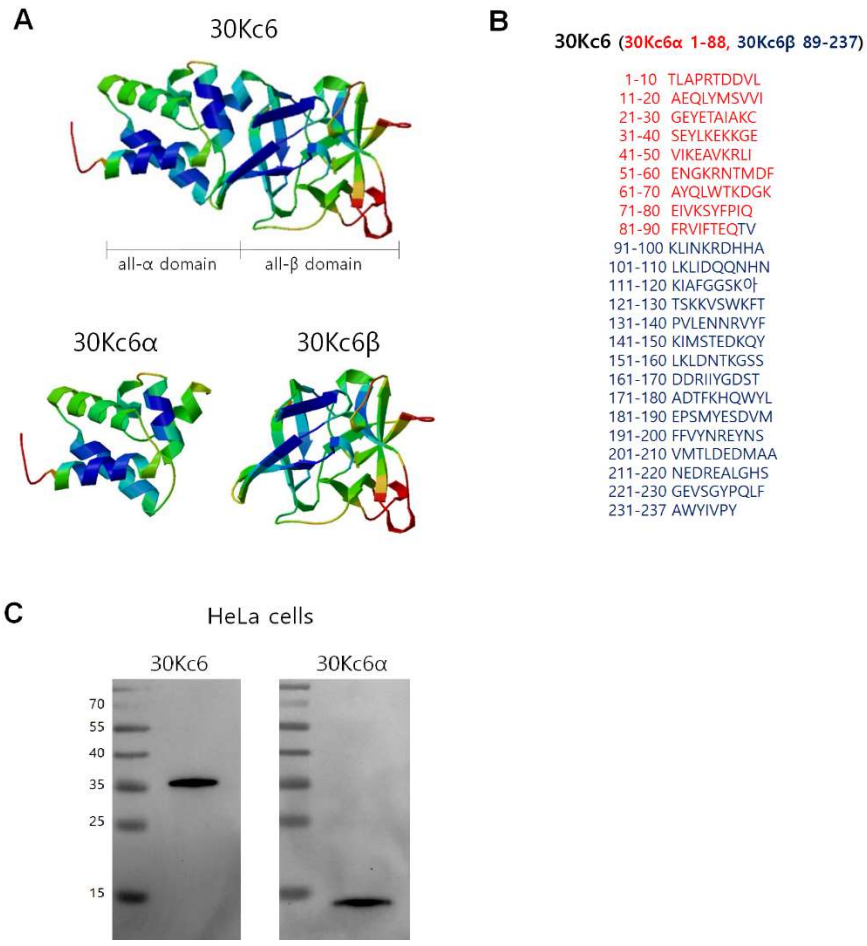

Figure 5.2 The structure of 30Kc6 and protein expression

A. 30Kc6 protein was truncated into N-terminal alpha-helix (30Kc6 α), and C-terminal beta-sheet (30Kc6 β) regions. B. Amino acid sequences of 30Kc6 α. C. Gene expression of 30Kc6 and 30Kc6 α in cells.

5.3 Anti-apoptosis property of 30Kc6α

To analyze apoptotic property of 30Kc6α, cells were transfected with 30Kc6 or 30Kc6α. One μM of STS was treated to cells for 5 h, then the cells were further incubation for 24 h with fresh media. From FACS analysis, although the percentage of apoptotic cells in control was 77.85, there were shown 53.29% in 30Kc6-transfected cells, and 44.52% in 30Kc6α-transfected cells, n=3 (Figure 5.3 A). It was relatively low percentage in early apoptotic cells; the apoptotic cells in control were 39.73%, and 30Kc6- or 30Kc6α-transfected cells were 17.74% or 11.78%. Interestingly, in late apoptotic cells, 30Kc6α-transfected cells were observed the lower apoptotic percentage than 30Kc6-transfected cells (Figure 5.3 B). This results indicate that 30Kc6α had similar or higher effect on anti-apoptosis comparing with 30Kc6. However, we did not observe anti-apoptotic effect on primary cell, due to the low transfection efficiency. To solve low transfection efficiency of some cells, we tried to produce 30Kc6α protein with 30Kc19 cell-penetrating protein.

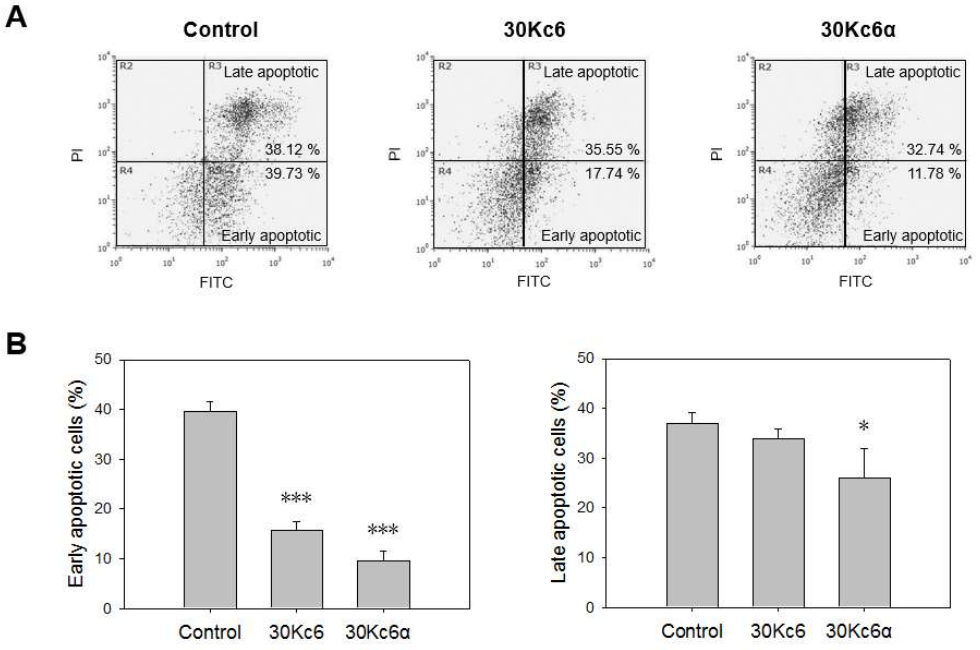

Figure 5.3 Anti-apoptotic property of 30Kc6α

A. Analysis of apoptotic cells by FACS. B. Early and late apoptosis shown as histograms. *$p < 0.05$, ***$p < 0.001$ compared with the control group (n = 3). Error bars represent standard deviation.

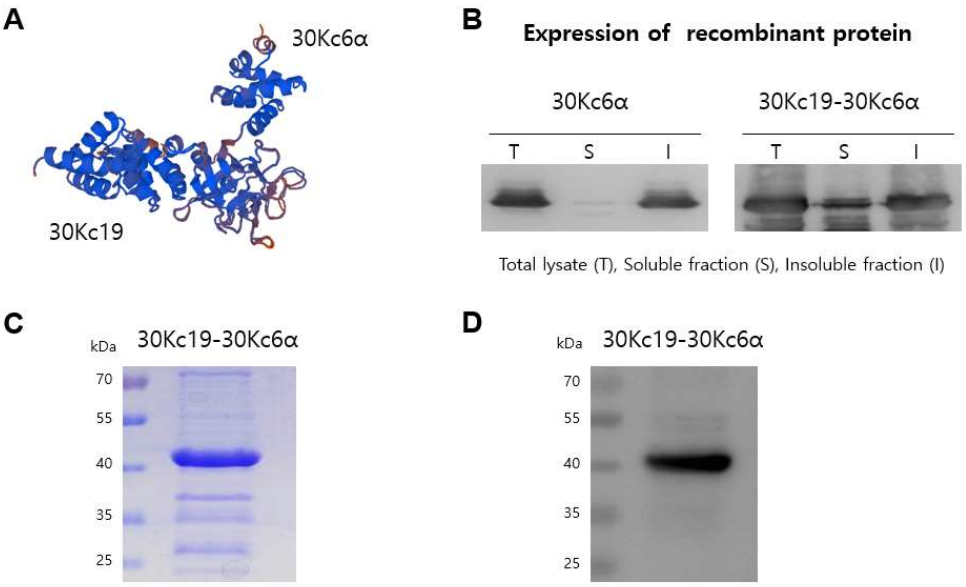

Figure 5.4 Expression and purification of 30Kc19-30Kc6α

A. The structure of 30Kc19-30Kc6α. B. Expression of recombinant 30Kc19-30Kc6α protein. C. Coomassie blue staining of purified soluble 30Kc19-30Kc6α protein, and Western blot analysis (D).

5.4 Expression and purification of 30Kc19-30Kc6α protein

To enter the cells, 30Kc6 was conjugated genetically with 30Kc19 cell-penetrating protein (Figure 5.4 A). 30Kc19 cloned vector was gained our previous study [15]. 30Kc19 has cell-penetrating and neighbor proteins-stabilizing properties [20, 73]. 30Kc6α was expressed aggregation form, inclusion body, from *E. coli*. However, when 30Kc19 was conjugated, 30Kc6α was expressed as a soluble form (Figure 5.4 B). Thus, 30Kc19-30Kc6α protein was expressed, and purified by FPLC. Purified soluble 30Kc19-30Kc6α proteins were separated by SDS-PAGE, and analyzed by Coomassie blue staining (Figure 5.4 C) and Western blot (Figure 5.4 D). Thus, recombinant 30Kc19-30Kc6α protein was expressed as soluble and the protein band was observed in proper size, about 43 kDa.

5.5 Cytotoxicity and cell penetration of 30Kc19-30Kc6α protein

Cytotoxicity test was performed by CCK-8 assay. 30Kc19-30Kc6α proteins were added 10, 20, 30, and 40 μM in the cell medium. After 24 h incubation, HeLa cells were analyzed. Although

10 and 20 μM of proteins had not relatively decrease in cell viability, 30 and 40 μM of proteins showed about 85% cell viability (Figure 5.5 A). Thus, for further use, the concentration of protein was considered lower than 30 μM.

For observation of cellular penetration for recombinant proteins, we analyzed cells by immunocytochemistry. When the cells were incubated with 0.25 μM (10 μg/ml) of 30Kc19-30Kc6α for 24 h, the proteins were observed in cells. However, the same concentration of 30Kc6α protein was not entered the cells (Figure 5.5 B). Then, we checked whether 30Kc19-30Kc6α proteins are in cytosol using confocal microscopy. On figure 5.5 C, 10 μM of 30Kc19-30Kc6α protein was observed in cytosol. Thus, 30Kc19 protein could drag 30Kc6α into cells.

5.6 Anti-apoptotic property of 30Kc19-30Kc6α protein

Anti-apoptotic effect of 30Kc19-30Kc6α was tested. The day before apoptosis induction, 10 or 40 μM of 30Kc19-30Kc6α proteins were added in cells for 24 h. To induce apoptosis, the cells were incubated with 1 μM STS for 5 h. Apoptotic cells were stained by Annexin V-FITC, and analyzed by FACS (Figure 5.6 A). When

10 or 40 μM of 30Kc19-30Kc6α protein was added, the percentage in early apoptotic cell was 11.75 or 11.48. It was decrease about 25.7 or 26% comparing with control. Interestingly, in late apoptosis, cells with 40 μM of 30Kc19-30Kc6α protein were 20.5% lower than cell with none (control), also 11.5% lower than cells with 10 μM of protein (Figure 5.6 B). Although cytotoxicity for 40 μM of protein was observed (Figure 5.5 A), total viability of cells with 40 μM of protein was increased comparing with that with 10 μM of protein. the results indicate that 30Kc19-30Kc6α protein had anti-apoptotic properties, and the effect on anti-apoptosis was dependent on the concentration of protein.

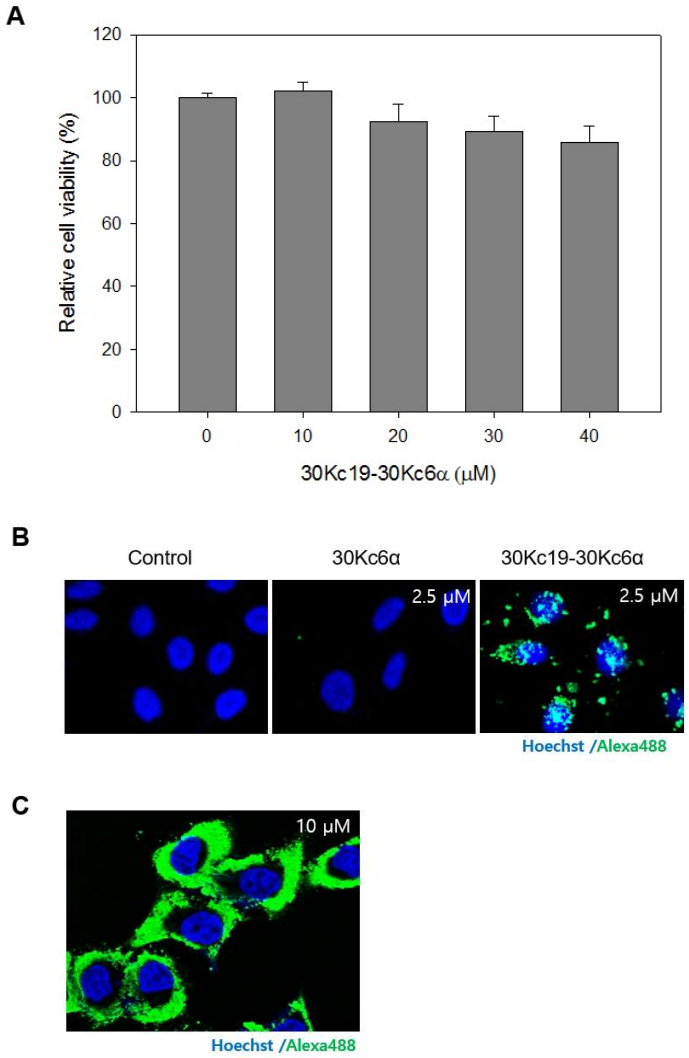

Figure 5.5 Cytotoxicity and penetration of 30Kc19-30Kc6α

A. Cytotoxicity analysis by CCK-8 assay. The cells were incubated with proteins for 24 h. Error bars represent standard deviation. (n = 3) B. 2.5 μM 30Kc19-30Kc6α protein was observed in cells. C. Cells with 10 μM protein were analyzed by confocal microscope.

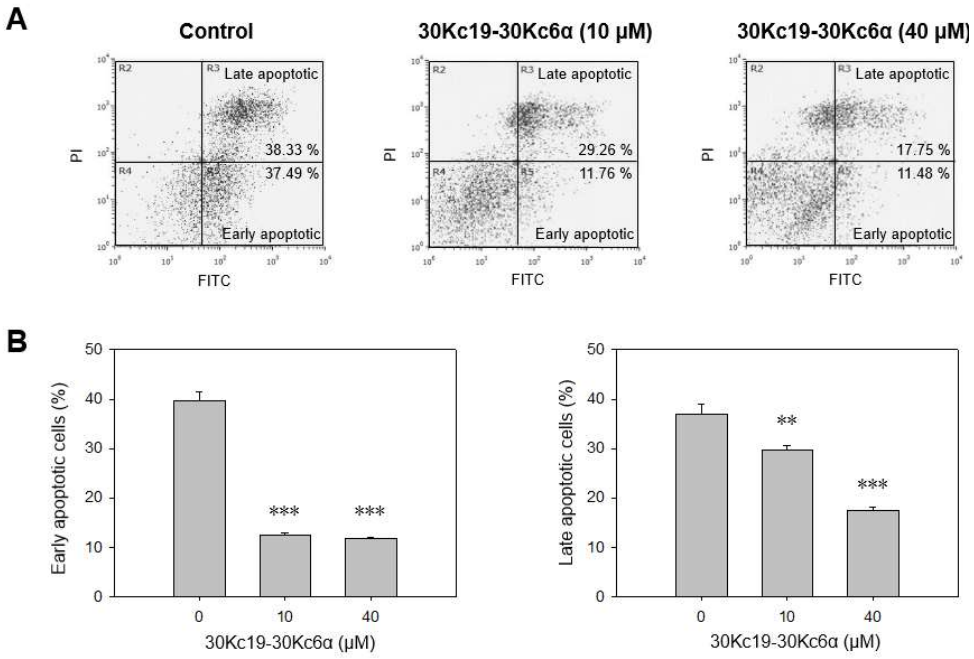

Figure 5.6 Anti-apoptotic property of 30Kc19-30Kc6α protein

A. Analysis of apoptotic cells by FACS. B. Early and late apoptosis shown as histograms. $^{**}p < 0.01$, $^{***}p < 0.001$ compared with the control group (n = 3). Error bars represent standard deviation.

5.7 Conclusions

Inhibition of apoptosis plays an important role for a treatment of many diseases such as Parkinson's and Alzheimer's disease. In our previous research, 30Kc6 proteins derived from silkworm hemolymph have been revealed as anti-apoptosis proteins in mammalian cells. 30Kc6 proteins are distinct two regions; N-terminal all-alpha region and C-terminal all-beta region. We considered that alpha-helix regions of 30Kc6 proteins are a major part to take an anti-apoptotic property.

In this study, we cloned 30Kc6 alpha (30Kc6α) to a mammalian expression vector, and the vector was transfected to cells. Then, gene transfected cells were induced apoptosis using Staurosporine (STS). From the analysis of Annexin V-FITC stained cells, the percentage of apoptotic cells in 30Kc6α was lower than that in 30Kc6 or control.

Furthermore, when 30Kc6α was expressed as proteins with 30Kc19, recombinant 30Kc19-30Kc6α protein could express as soluble, and penetrate into cells. Lastly, 30Kc19-30Kc6α protein showed anti-apoptotic property. In this study, we investigated that

30Kc6α plays role in anti-apoptosis which whole 30Kc6 has. Furthermore, 30Kc19-30Kc6α protein had anti-apoptotic property by penetrating into cells. Thus, we anticipated 30Kc6α to be used for many study in apoptosis.

Chapter 6.

Soluble expression and stability enhancement of transcription factors using 30Kc19 cell-penetrating protein

Chapter 6. Soluble expression and stability enhancement of transcription factors using 30Kc19 cell-penetrating protein

6.1 Introduction

A transcription factor is known as a regulator that localizes into the nucleus and controls gene expression by binding to specific DNA sequences [74]. Since the generation of induced pluripotent stem cells (iPSCs) using four defined transcription factors (Oct4, Sox2, c-Myc, and Klf4), many have taken an interest because transcription factors have clinical significance as a therapeutic gene modulator [23, 24]. However, a virus-based approach may cause tumorigenicity due to integration into the host cell genome [75]. As a solution, there have been many trials to evade viral transduction by using non integrating plasmids [76]. PiggyBac transposons [77]. and small-molecule compounds [78]. Although plasmids and transposons can reduce the risks, they still have potency for genomic integration. Besides, molecule compounds were able to reprogram mouse cells but were insufficient in reprograming human cells. Thus, a protein-

based approach is a practical method for clinical use that can limit safety risks and has many advantages [60].

There were many trials to express transcription factors as recombinant proteins for the exploration of their mechanisms and the application as clinical drugs [79]. *Escherichia coli* (*E. coli*) has been used commonly for the production of recombinant proteins due to its high productivity, low production cost, and ease of product isolation [80]. However, there are some technical bottlenecks in the production of transcription factor from *E. coli*. For instance, the recombinant proteins are expressed as aggregate forms in many cases. As a result, it requires additional solubilization and refolding steps which increases production cost and decreases yield [81]. In addition, there is the risk that the protein may lose the original bioactivity after the refolding process [82, 83]. Methods to increase solubility have been reported by optimizing *E. coli* culture conditions [84]or through the use of a buffer system [85].

In our previous study, 30Kc19 protein derived from *Bombyx mori*, delivered protein cargos into cells [16] by a dimerization mechanism [17] and enhanced enzyme stability [19, 20, 73]. Here, we have used 30Kc19 cell-penetrating protein as a novel fusion partner of

transcription factors which can be used in protein-based iPSC generation. We anticipate that a 30Kc19 protein could deliver a transcription factor into cells and also solve problems that normally arise in the production of transcription factors, such as low soluble expression and protein instability. Thus, we propose that the multifunctional properties of 30Kc19 protein can be applied to general transcription factors and overcome several hurdles when used as recombinant proteins.

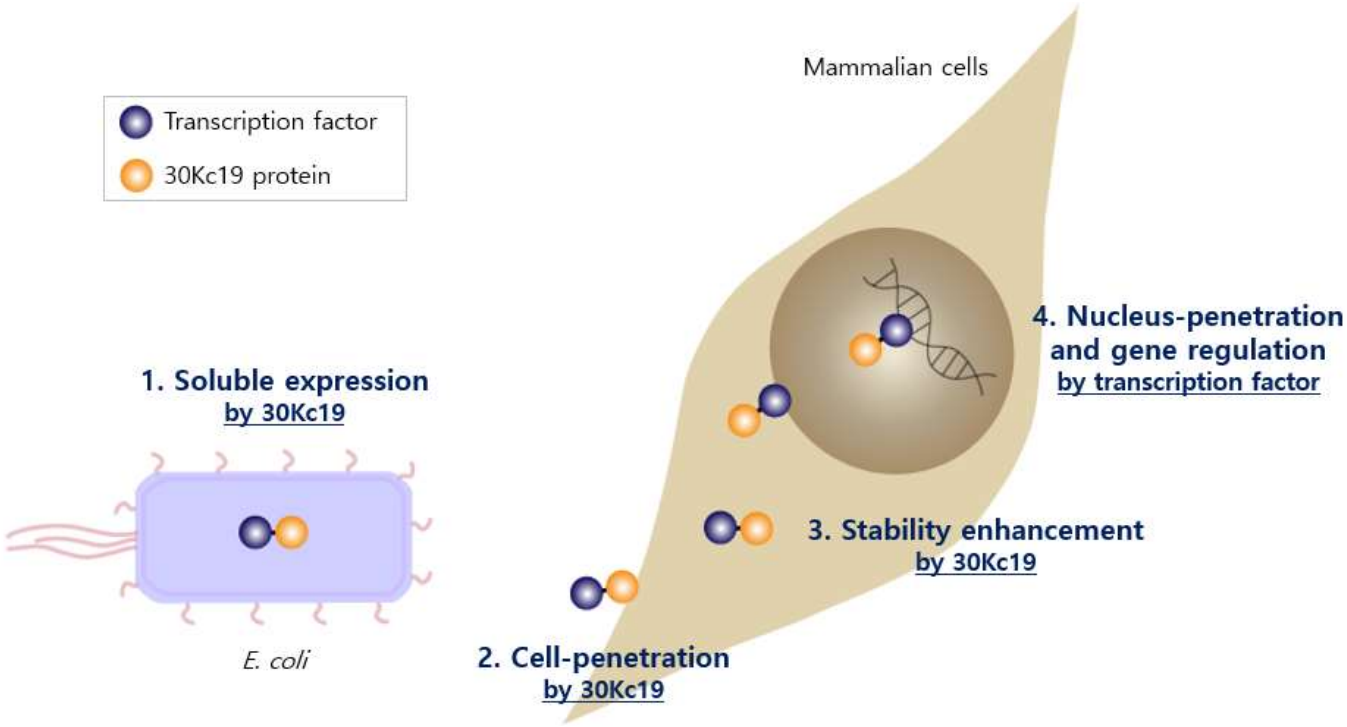

Figure 6.1 A schematic illustration of gene regulation by transcription factor−conjugated 30Kc19 protein

6.2 Soluble expression and purification of transcription factors

First of all, the effect of 30Kc19 protein conjugation to transcription factors on soluble expression was determined (Figure 6.2). Transcription factors were cloned in the pET23a vector for recombinant protein expression in *E. coli*. Each factor was comprised with a T7 tag at the N-terminus for immunoassay and a His tag at the C-terminus for purification using affinity chromatography (Figure 6.2 A). For the delivery of protein into cells, each factor was fused with nine-arginine (R9) or 30Kc19. Transcription factor alone or with 30Kc19 was expressed in *E. coli*, and the lysates were separated into soluble and insoluble fractions. Total lysate and soluble fraction were then analyzed by SDS-PAGE and Western blot. In previous studies, most transcription factors were demonstrated to have poor solubility and require a solubilization process [40, 86, 87]. When Oct4 alone was expressed, it was expressed mainly as an inclusion body, and the level of soluble form was extremely low (Figure 6.2 B). Interestingly, a considerable amount of Oct4 conjugated with 30Kc19 protein was expressed in soluble fraction, meaning that 30Kc19 protein enhanced soluble expression. For Sox2 and Klf4, we observed that some of those transcription factors were

expressed as soluble proteins in our expression system as shown in Figure 6.2 B. The relative protein expression level of each protein is shown in Figure 6.2 C.

To assess the effect of CPPs (R9 and 30Kc19) on soluble expression, transcription factors conjugated with R9 or 30Kc19 were expressed at 27 or 37℃ and the soluble fraction of each protein was analyzed by Western blot. As shown in Figure 6.2 C, 30Kc19 promoted the production of Oct4 more as a soluble protein when expressed at either 27 or 37℃, while R9 did not influence Oct4 solubilization. Sox2 and Klf4 were expressed as soluble proteins regardless of CPP type (Figure 6.2 C). While c-Myc was expressed as insoluble protein in any situation, another Myc family member, L-Myc [88, 89], was highly expressed as a soluble protein when it was fused with 30Kc19 protein, whereas L-Myc alone showed a lower expression level and was not produced in soluble form. With R9, a small amount of L-Myc was expressed as soluble protein at 27℃. Overall, these results demonstrate that 30Kc19 protein enhanced the soluble expression of Oct4, Sox2, and L-Myc, which became 7.0, 2.9, and 23.8 times its original amount, respectively.

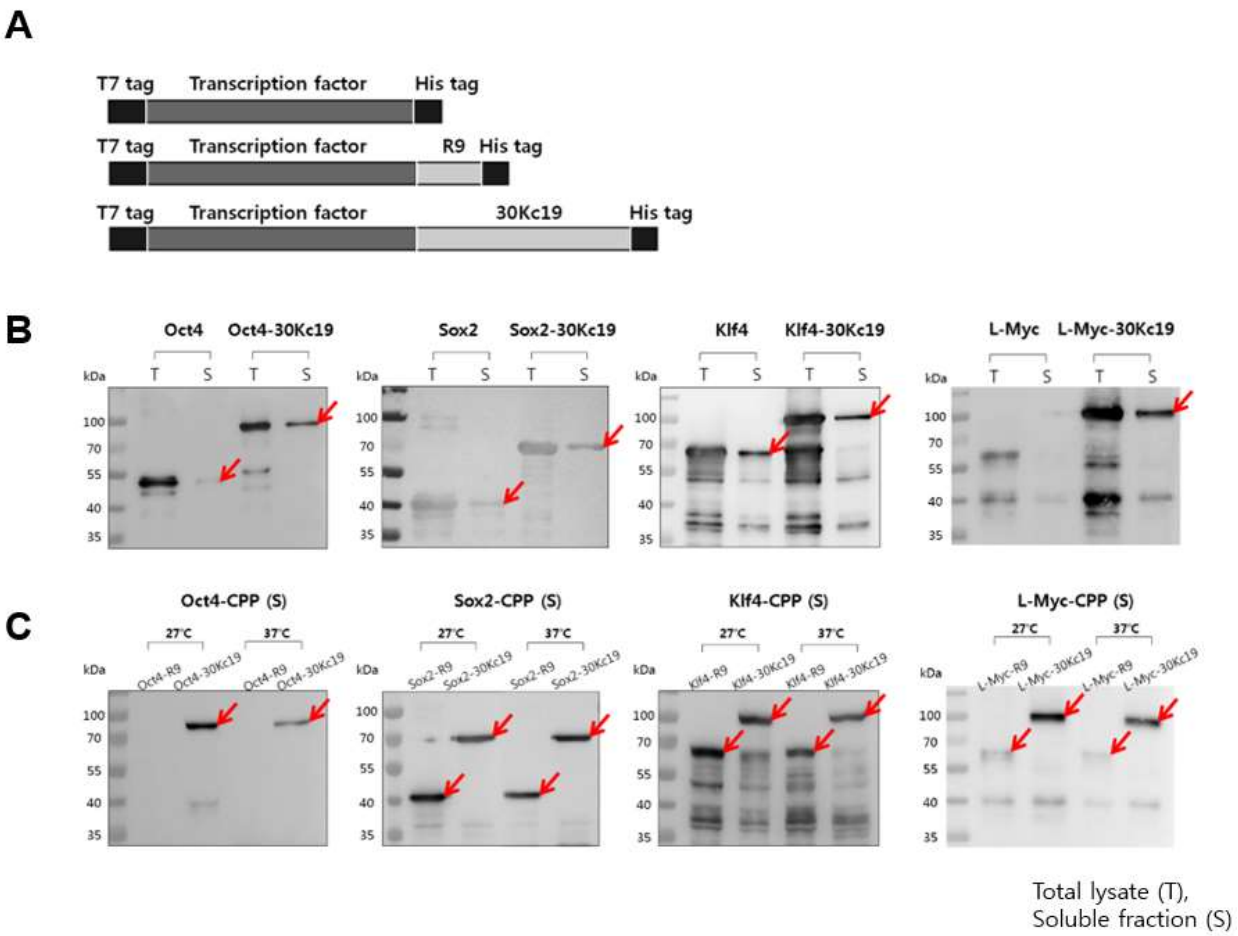
A
T7 tag
Transcription factor
His tag
T7 tag
Transcription factor
R9
His tag
T7 tag
Transcription factor
30Kc19
His tag
B
Oct4
Oct4-30Kc19
Sox2
Sox2-30Kc19
Klf4
Klf4-30Kc19
L-Myc
L-Myc-30Kc19
kDa
T
S
100
70
55
40
35
C
Oct4-CPP (S)
Sox2-CPP (S)
Klf4-CPP (S)
L-Myc-CPP (S)
27°C
37°C
Oct4-R9
Oct4-30Kc19
Sox2-R9
Sox2-30Kc19
Klf4-R9
Klf4-30Kc19
L-Myc-R9
L-Myc-30Kc19
Total lysate (T),
Soluble fraction (S)

Figure 6.2 Plasmid construction and soluble expression of transcription factors

A. Transcription factors (Oct4, Sox2, c-Myc, Klf4, and L-Myc) were developed with and without nine arginine (R9) or 30Kc19. **B.** Comparison of soluble expression between transcription factors alone and transcription factors-30Kc19 at 37℃. *E. coli* lysates were analyzed by Western blot. T total lysate, S soluble fraction. **C.** The effect of a CPP for solubilization of transcription factors at 27 and 37℃. Soluble fractions were analyzed by Western blot. The arrows indicate soluble target proteins.

6.3 Analysis of purified soluble transcription factors

To further explore the role of the 30Kc19 protein conjugation on recombinant transcription factors, soluble transcription factors were purified using affinity chromatography. The size and amount of purified soluble proteins were confirmed by Coomassie blue staining (Figure 6.3 A) or Western blot (Figure 6.3 B). As shown in Figure 6.3, each of the purified proteins was confirmed for their proper size. The results of purified Oct4 alone are not shown as there was insufficient amount of original soluble Oct4 as mentioned in Figure 6.2. The amounts of purified soluble Sox2 and Klf4, without any conjugations, were also low. In contrast, a relatively high level of purified soluble Oct4-30Kc19, Sox2-30Kc19, and Klf4-30Kc19 was observed, which coincides with the results in Figure 6.2.

6.4 *In vitro* stability of soluble transcription factors

The stability of transcription factors is important for effective gene regulation during cell culture. Here, we have investigated if 30Kc19 protein conjugation contributes to the stability of transcription factors. To test the effect of 30Kc19 protein on the stability of soluble transcription factors in solution, seven purified soluble

transcription factors (Oct4-30Kc19, Sox2, Sox2-R9, Sox2-30Kc19, Klf4, Klf4-R9, and Klf4-30Kc19) were added and incubated in the culture medium. Oct4 alone and Oct4-R9 were ruled out as they were expressed as an inclusion body resulting in negligible amount of soluble proteins. In serum-free medium, 10-15 μg/ml of purified soluble transcription factors were incubated at 37℃ for 24 or 48 h before analysis. By using 30Kc19 protein as a fusion partner for transcription factors, we found that the stability of the soluble transcription factors was significantly increased (Figure 6.4). The levels of Sox2 and Klf4 proteins produced alone or with R9 drastically decreased even within 24 h of incubation in medium, indicating poor stability. In contrast, all the transcription factors conjugated with 30Kc19 protein were stable for 48 h of incubation. Thus, it is conclusive that the conjugation of 30Kc19 protein enhanced the stability of transcription factors in the medium.

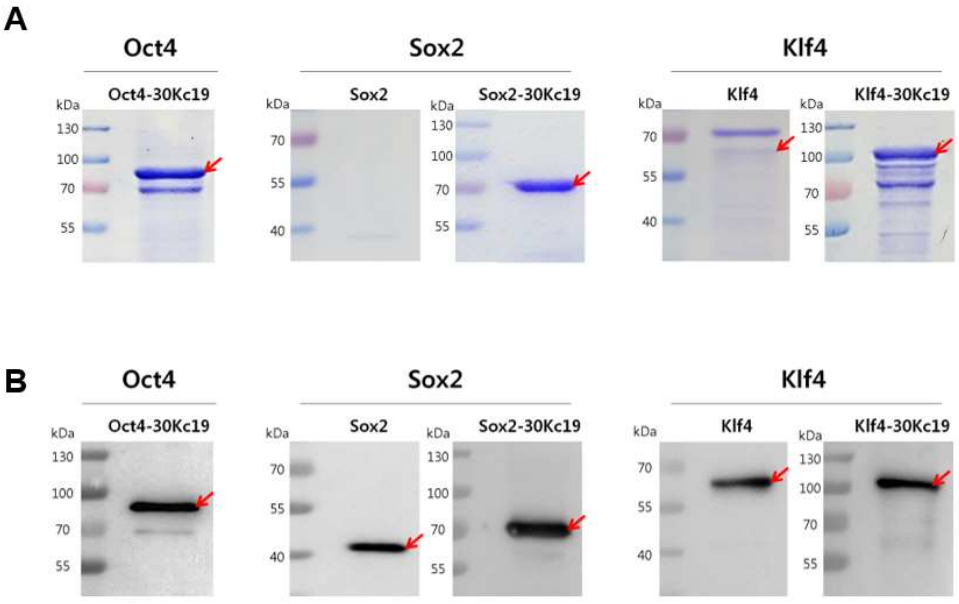

Figure 6.3 SDS-PAGE and Western blot analysis of purified soluble transcription factors

Soluble transcription factors were purified using affinity chromatography. Purified proteins were separated by SDS-PAGE then visualized using Coomassie blue staining (A) or Western blot (B). The arrows indicate target proteins.

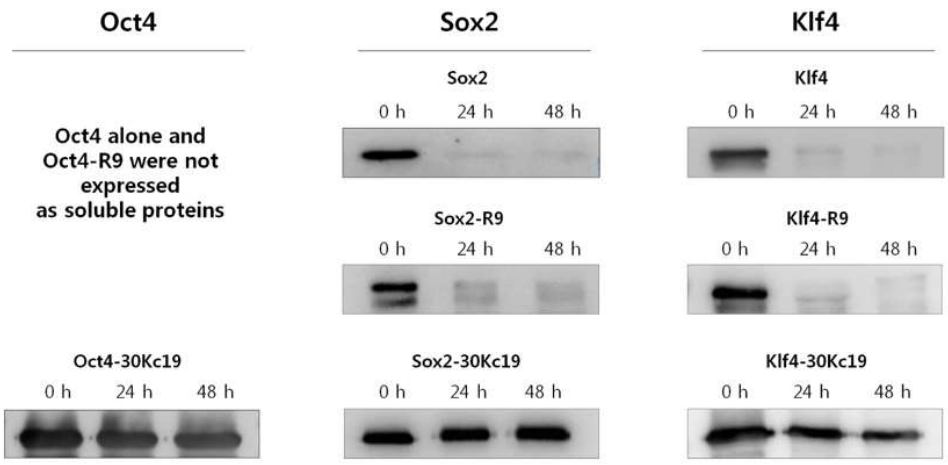

Figure 6.4 *In vitro* stability of soluble transcription factors.

A. Purified Oct4-30Kc19 soluble protein was incubated in serum-free media at 37℃ and analyzed using Western blot. The results of Oct4 alone and Oct4-R9 are not shown as they were expressed as aggregate forms. B, C. Purified Sox2 and Klf4 soluble protein were incubated with and without CPPs in serum free media at 37℃. After incubation for the indicated periods of time, the protein was analyzed by Western blot. Note that 30Kc19-conjugated transcription factors remained intact even at 48 h of incubation

6.5 Cell penetration and intracellular stability of soluble transcription factors

In our previous work, 30Kc19 protein delivered cargo protein into various cells and organs with maintaining its stability and causing low cytotoxicity [16]. Thus, the 30Kc19-conjugated transcription factors were selected for further study based on the following expectations: enhanced intracellular delivery and stability, and low cytotoxicity. First, the cell-penetration property of soluble transcription factors with 30Kc19 proteins was observed. To monitor the penetration of transcription factors into HDF cells, the proteins were labeled with Alexa Fluor® 488 and added to a culture medium at 20 μg/ml of the concentration. The fluorescence was observed in a live cell image using confocal microscopy. As shown in Figure 6.5 A, the transcription factor with the 30Kc19 protein was observed in the cells within 30 min of incubation, and its intracellular concentration gradually increased over time. This indicates that 30Kc19 protein conjugation successfully delivered transcription factors into cells.

To confirm how long 30Kc19-conjugated transcription factors remain in the cells, intracellular stability was observed by

immunofluorescence analysis. We added 10 μg/ml of transcription factors to HDF cells for 24 and 48 h, respectively, and then the delivered proteins in the cells were detected with immunofluorescence. 30Kc19-conjugated transcription factors appeared to be stable inside the cells for up to 48 h (Figure 6.5 B). These results show that 30Kc19-conjugated transcription factors were stable in the cells and also agree with the in vitro results.

6.6 Cytotoxicity of 30Kc19-conjugated transcription factors

Subsequently, we evaluated if 30Kc19-conjugated transcription factor has cytotoxicity. HDF cells were treated with the same concentration of four conjugated transcription factors simultaneously for 12 and 24 h in a dose-dependent manner, and then cell viabilities were assessed using MTT assay (Figure 6.6). The concentration of each protein was 2, 5, 10, and 15 μg/ml, respectively. Even when the cells were treated with 60 μg/ml of four conjugated transcription factors (15 μg/ml each), there was no decrease in cell viability, meaning that 30Kc19-conjugated transcription factors have low cytotoxicity.

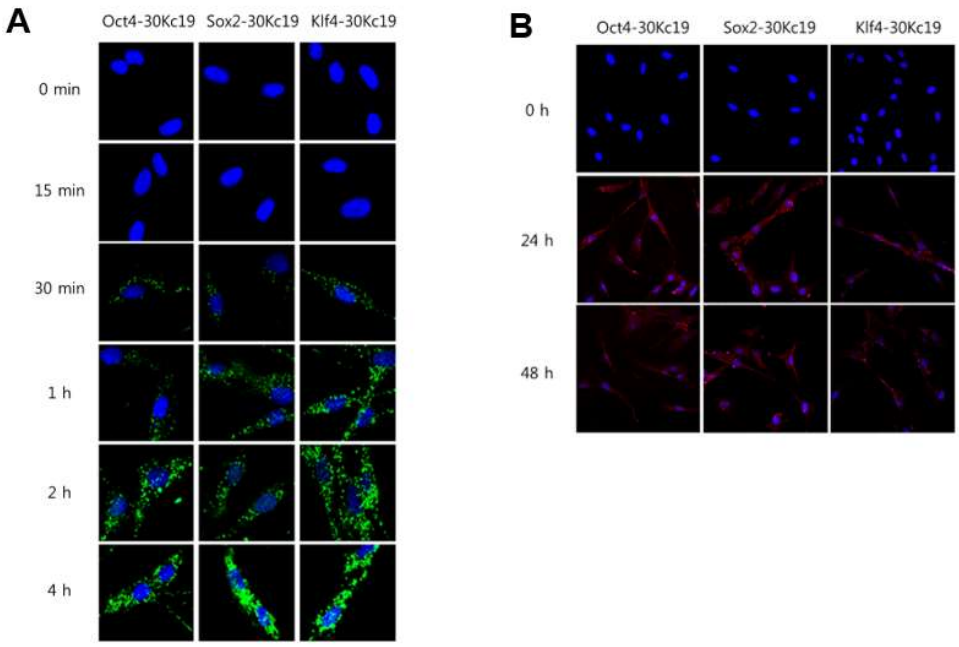

Figure 6.5 Cell-penetrating property of 30Kc19-conjugated soluble transcription factors

A. Proteins were labeled with Alexa Fluor 488 (green) for live cell imaging of 30Kc19-conjugated transcription factors (Oct4, Sox2, and Klf4). HDF cells were treated with labeled proteins in a time-dependent manner and detected using confocal microscopy. **B.** Intracellular proteins after incubation were analyzed by immunofluorescence. Alexa Fluor 594 (red) antibody for target proteins was used for the detection of transcription factors in the cells. Nuclei were visualized by Hoechst (blue).

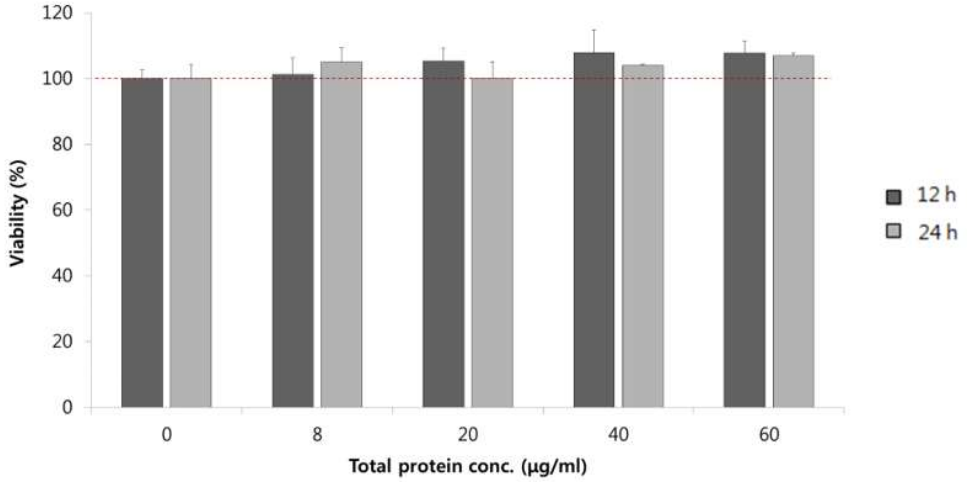

Figure 6.6 Cellular toxicity test for transcription factors

Cytotoxicity of 30Kc19-conjugated transcription factors. Four transcription factors were combined and cell viabilities were measured by MTT assay. HDF cells were treated with 2, 5, 10 and 15 μg/ml of each protein (Oct4-30Kc19, Sox2-30Kc19, c-Myc-30Kc19 and Klf4-30Kc19) for 12 and 24 h. Total protein= Oct4-30Kc19 + Sox2-30Kc19 + c-Myc-30Kc19 + Klf4-30Kc19. Error bars represent standard deviation. (n = 3)

6.7 Transcriptional activity of 30Kc19−conjugated Klf4

Once introduced into cells, a transcription factor binds to its target DNA sequence in the nucleus for the control of transcription. Thus, we tested the transcriptional activity of a transcription factor−conjugated with 30Kc19 protein compared with that conjugated with R9. Among transcription factors, Klf4 protein was chosen to confirm whether our recombinant proteins have transcriptional activity in the cells. When cells were treated with Klf4−30Kc19 protein, luciferase activity increased significantly depending on the concentration (Figure 6.6 A). Then, the transcriptional activity of Klf4−conjugated with 30Kc19 or R9 was compared. One micrograms per milliliter of each transcription factor was delivered, and transcriptional activities were measured 4 and 24 h after delivery. Klf4−30Kc19 increased transcriptional activity ($p < 0.05$) as time progressed (Figure 6.6 B). In contrast, there was no significant increase in transcriptional activity of Klf4−R9 (p = nonsignificant; NS). We can hypothesize that the higher transcriptional activity of Klf4−30Kc19 was due to the increased intracellular stability of Klf4 through 30Kc19 conjugation. Immunocytochemistry of intracellular Klf4−30Kc19 and Klf4−R9 showed that Klf4−R9 level in cells drastically decreased

from 4 to 24 h after delivery (Figure 6.6 C). In contrast, there was a considerable amount of Klf4-30Kc19 still in the cells even at 24 h after delivery. This observation was similar to the *in vitro* stability results shown in Figure 6.4. Thus, it is obvious that 30Kc19 conjugation enhanced transcriptional activity by increasing the intracellular stability of a transcription factor.

6.8 Conclusions

In this study, we have used 30Kc19 cell-penetrating protein as a novel fusion partner of transcription factors which can be used in protein-based iPSC generation. It was hypothesized that the 30Kc19 protein has the potential to be developed as a fusion partner in the protein-based delivery of transcription factors for the regulation of gene expression, as it was shown to enhance the intracellular delivery as well as stability of its fusion protein. Interestingly, we have also found that the C-terminal fusion of the 30Kc19 protein promoted the soluble production of transcription factors, especially for Oct4 and L-Myc, while R9 did not.

Also, we have shown that a 30Kc19 cell-penetrating protein simultaneously enhances soluble expression, stability, and the

transcriptional activity of transcription factors. Therefore, we propose that the multifunctional properties of 30Kc19 protein can be applied to general transcription factors and overcome several hurdles when used as recombinant proteins.

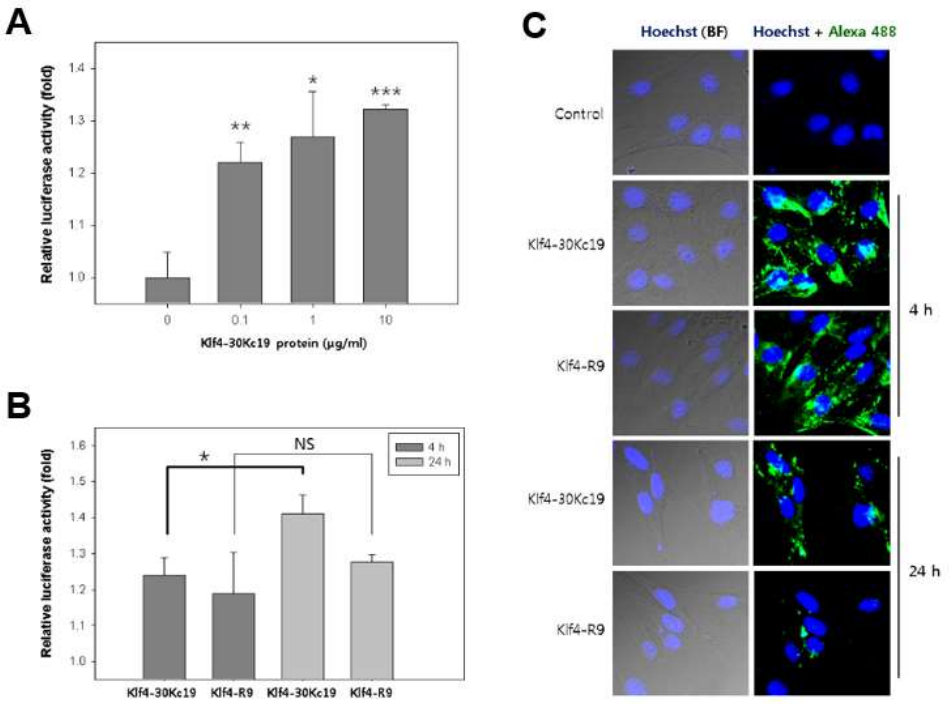

Figure 6.7 Effect of 30Kc19 conjugation on intracellular transcriptional activity of Klf4 protein

A. Klf4-30Kc19 protein was delivered into transfected cells, and luciferase activity was measured after 4 h to determine transcriptional activity. $*p < 0.05$, $**p < 0.01$, $***p < 0.001$ compared with the control group (n = 3). Error bars represent standard

deviation. **B.** One micrograms per milliliter of Klf4-R9 or Klf4-30Kc19 proteins were added to cells. Luciferase activity of Klf4 was measured after 4 or 24 h incubation, respectively. (*$p < 0.05$, NS nonsignificant). **C.** Delivered Klf4 protein with 30Kc19 or R9 was analyzed by immunofluorescence. Green fluorescence represents the amount of Klf4 protein in the cells. Bright field (BF) images and fluorescence of nuclei (blue) images were merged and shown in the left panel. The numbers indicate the time of incubation.

Chapter 7.

Direct conversion of fibroblasts to neuronal cells by 30Kc19-Ascl1-NLS-R9 protein

Chapter 7. Direct conversion of fibroblasts to neuronal cells by 30Kc19-Ascl1-NLS-R9 protein

7.1 Introduction

Direct conversion, which is also known as transdifferentiation, has been actively developed due to rapid process with high efficiency. For cellular conversion, specific transcription factors were found, and they induced somatic cells to desired cells such as myoblasts [25], cardiomyocytes [26], pancreatic beta cells [27], or neurons [29]. For neuron conversion, recent work has shown that forced expression of a combination of 3 reprogramming factors, Ascl1, Brn2 (also known as Pou3f2), Myt1l can efficiently convert mouse fibroblasts into functional induced neuronal cells (iNCs) [29]. A year later, the group then showed that using Ascl1 alone, generated functional iNCs from mouse and human fibroblasts (MEFs, HFFs), indicating that Ascl1 is the key driver for reprogramming to iNCs, and that Myt1l and Brn2 are primarily for maturation purpose [90].

In this study, protein is applied for direct conversion in order to avoid safety risk of virus. Ascl1 is selected for the transcription factor of neural conversion,

Here, we have used 30Kc19 protein as a novel fusion partner of reprogramming factor Ascl1 for generation of protein-induced neuronal cells (p-iNCs). 30Kc19 protein can be used to solve a problem that normally arise in the production of reprogramming factors, such as protein instability and low soluble expression [80]. The 30Kc19-based transcription factor will be anticipated to be the new strategy for protein-based direct conversion.

7.2 Soluble expression of 30ANR protein

It was reported that 30Kc19 protein enhances soluble expression of reprogramming factors [73]. Hence, the effect of 30Kc19 protein conjugation to reprogramming factor Ascl1 on soluble expression was determined *30Kc19-Ascl1-NLS-R9* (*30ANR*) and *Ascl1-NLS-R9* (*ANR*) vectors were constructed into the pET23a expression vector system between the *Nhe*I and *Xho*I site (Figure 7.1 A). Each reprogramming protein was comprised with a T7 tag at the N-terminus for immunoassay. Both proteins were expressed in *E. coli* and then and the lysates were separated into soluble and insoluble fractions. Western blot analysis was performed by loading onto PAGE followed by an immunoblot against the His-tag, and

showed that fusion proteins were expressed correctly. Although 30ANR protein with a size of about 60 kDa was present in both soluble and insoluble fractions, ANR protein with a size of 37 kDa was only found in the insoluble fraction and not in the soluble fraction (Figure 7.1 B).

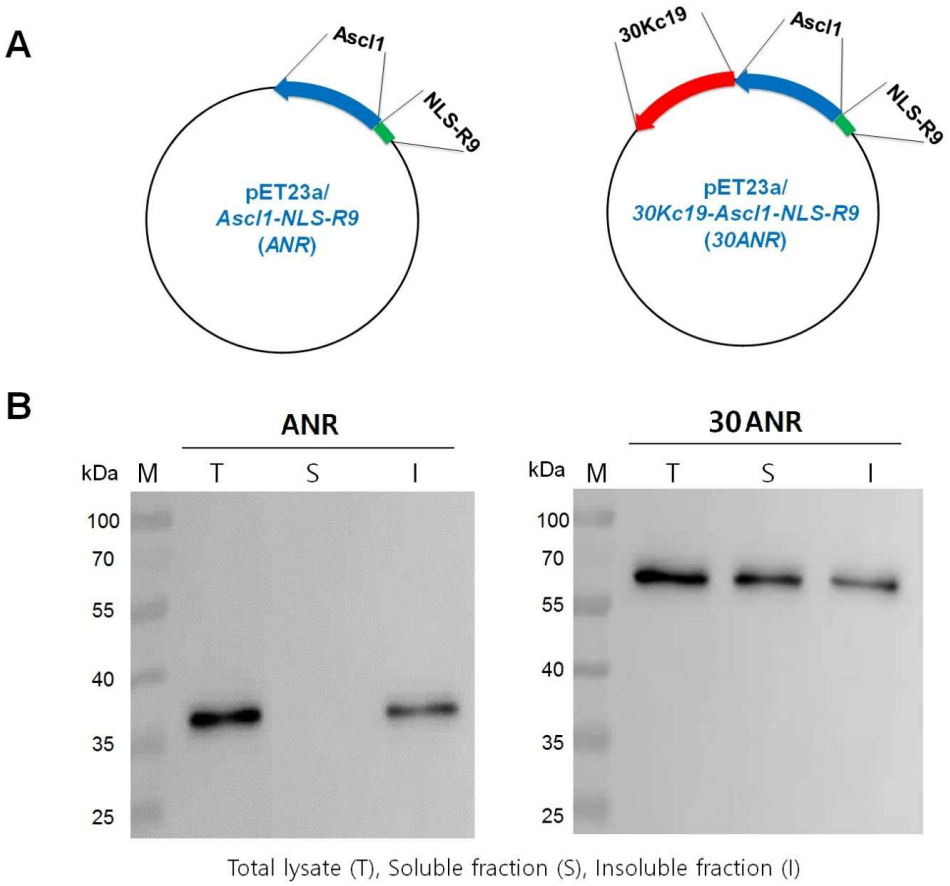

Figure 7.1 Gene cloning and soluble expression of ANR and 30ANR proteins

A. Cloning of 30ANR and ANR in pET23a vector. **B.** Protein expression pattern. 30ANR was expressed both soluble and insoluble proteins, although ANR was expressed only insoluble protein. Total lysate (T), soluble fraction (S), and insoluble fraction (I).

7.3 Purification, and *in vitro* stability of protein

Soluble 30ANR protein was purified by Fast Protein Liquid Chromatography (FPLC), then analyzed by SDS-PAGE Coomassie blue staining (Figure 7.2 A) and Western blot analysis (Figure 7.2 B). As demonstrated in Figure 7.2, 30Kc19 protein enhanced the soluble expression of the transcription factor, Ascl1. In previous study, 30Kc19 protein also enhanced the soluble expression of Oct4, Sox2, and L-myc proteins [73].

The stability of reprogramming factor is vital for effective gene regulation during cell development. Hence, we investigated the effect of 30Kc19 protein on the stability of Ascl1 protein. Purified soluble 30ANR protein was incubated in the serum-free culture medium at 37℃ and 5% CO_2 conditions and observed daily by Western blot analysis. ANR was ruled out as it was expressed as an inclusion body resulting in negligible amount of soluble proteins. By using 30Kc19 protein as a fusion partner for reprogramming factor, we found that the stability of the soluble reprogramming factors was significantly maintained. After 2 days, 50% of the protein was detected and after 3 days, still 40% of the protein was maintained (Figure 7.2 C).

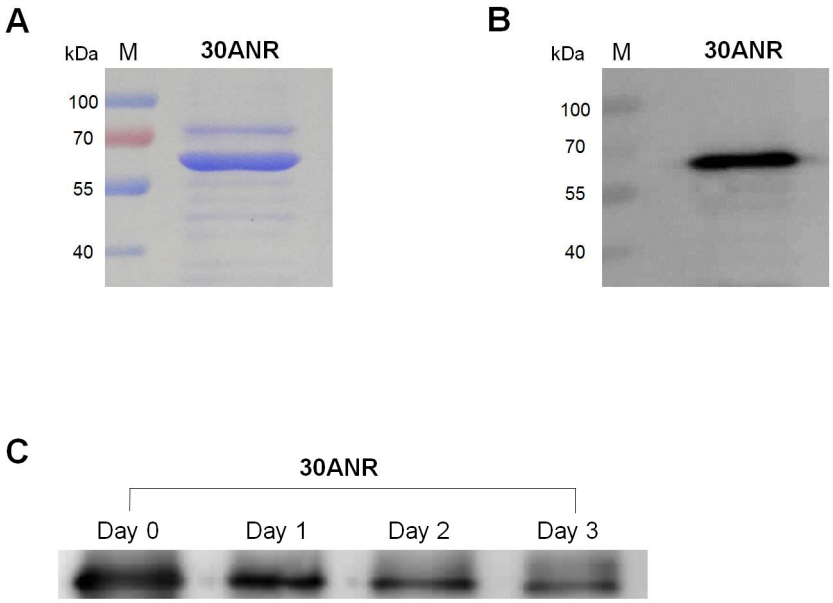

Figure 7.2 Soluble protein purification and *in vitro* stability of 30ANR protein

A. Analysis of purified soluble protein using Coomassie blue staining, and Western blot (**B**). The band size is about 60 kDa. **C.** *In vitro* protein stability test in serum-free media at 37℃. The soluble protein was collected for 3 days.

7.4 Cell penetration

Previously, we have observed delivery of cargo protein into various cells and organs using 30Kc19 protein [16]. Thus, soluble 30ANR protein was investigated for intracellular delivery. 50 μg/ml of fusion protein was added in mouse embryonic fibroblasts (MEFs) and incubated for 24 h at 37℃. Intracellular protein was analyzed by immunofluorescence using a confocal microscope. From Figure 7.3, 30ANR protein was observed in the cells. Generally, transcription factors have controlled gene using their little amount, although the protein was in nucleus, the fluorescent was faint. However, there were previous study about transcription factor which had faint fluorescence, but it had transcriptional activity [73].

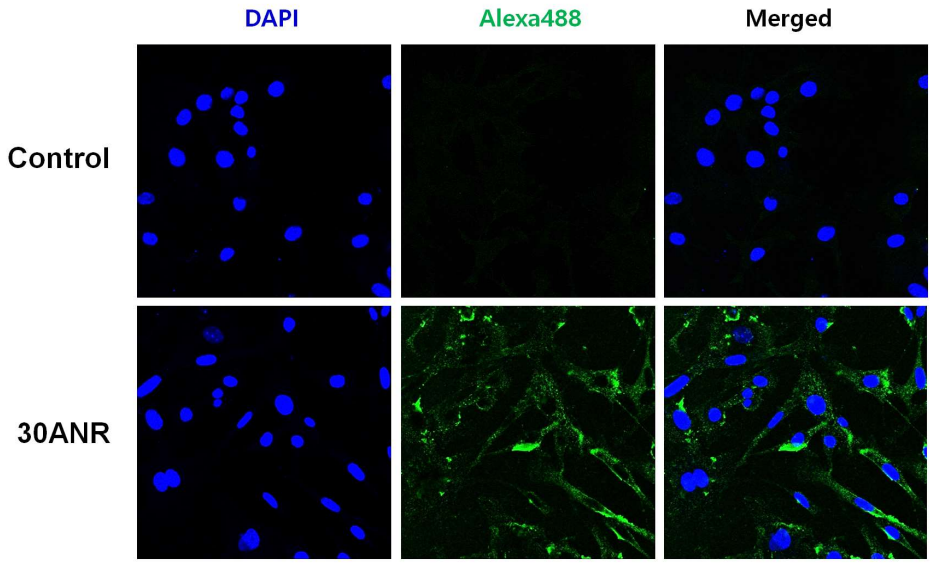

Figure 7.3 Cell penetration of 30ANR protein

MEFs were incubated with 50 μg/ml of 30ANR protein for 24 h. After incubation, the cells were analyzed confocal microscopy. Proteins were stained by Alexa488, and nucleus were stained by DAPI.

7.5 Cytotoxicity assay

Cytotoxicity of 30ANR protein was measured using CCK-8 assay (Figure 7.4). 30ANR protein showed negligible difference in the viability of cells, indicating no cytotoxicity in MEF for 0 - 90 μg/ml protein. $p > 0.05$ meant that these are statistically insignificant. Therefore, treatment of 30ANR exhibited no cytotoxicity on MEFs.

7.6 Generation of protein-induced neuronal cells (p-iNCs)

Previous co-culture of mouse embryonic cells (MEFs) and glial cells (astrocytes) study [90] was used in this study (Figure 7.5 A). To distinct between MEFs and astrocytes, MEFs were stained with viral DsRed (Figure 7.5 B). For co-culture, 2 x 10^5 MEFs and 2 x 10^4 astrocytes were seeded on 35 mm dish, and 50 μg/ml of proteins were treated on day 1 and 2 with DMEM-based MEF media. Then, from day 3, the cells were incubated with N3-based reprogramming media. In reprogramming media, proteins were treated to cells every 3 days because proteins are remained more than 50% until day 3. At day 7 and 14, the cell's morphology, gene expression.

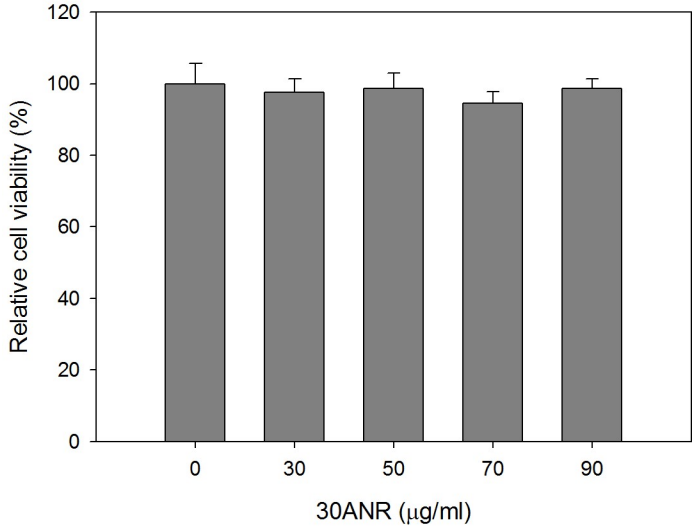

Figure 7.4 Cytotoxicity of 30ANR protein

Proteins were added into cell media, and cytotoxicity was analyzed by CCK-8 assay after 24 h incubation. Error bars represent standard deviation. (n = 3)

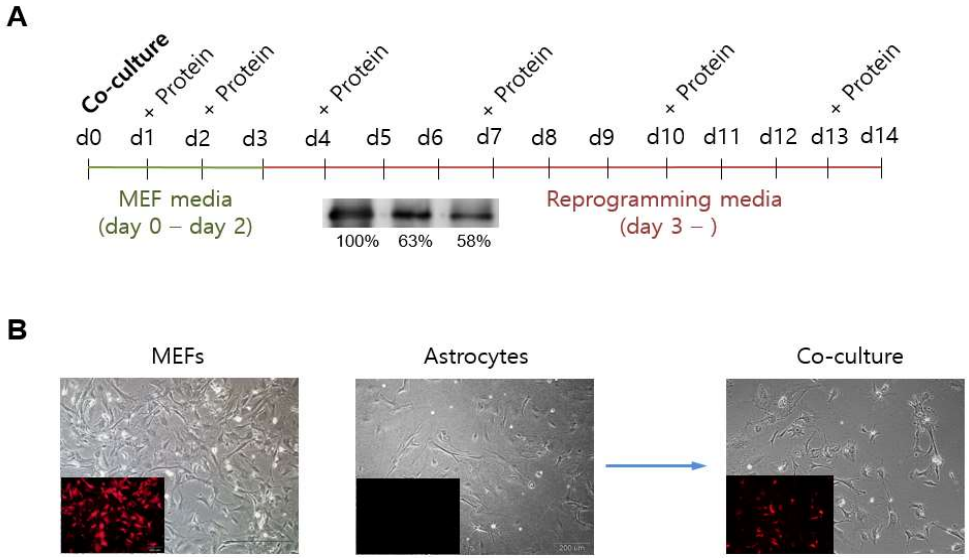

Figure 7.5 Schematic protocol for generating p-iNCs

A. Timeline for generating p-iNCs. For 3 days, MEFs and astrocytes were incubated in DMEM-based MEF media. Then, the cells were incubated in N3-based reprogramming media. The cells were treated with 30ANR protein 6 times for 14 days. B. MEFs were stained by viral DsRed, and in co-culture MEFs and astrocytes were distinguished easily.

7.7 Cell morphology change

From day 3, the changed cell morphologies were observed (Figure 7.6). Cells, that were cultured with 30ANR protein, showed difference in the cell morphology in comparison with the cells that were cultured without protein (Figure 7.6 A). To distinguish MEFs and Astrocytes, co-culture cells were analyzed by fluorescence microscopy. From the fluorescence image, cells which had long ends similar to the neuronal cells were MEFs which were stained by DsRed (Figure 7.6 B). Thus, 30ANR protein could change the morphology of MEFs.

7.8 Expression of neuronal biomarkers

For analysis of cells, neuron-specific class III beta-tubulin (Tuj1) and microtubule associated protein 2 (MAP2) were used (Figure 7.7). At day 7, in the protein treated dish, Tuj1 and MAP2 positive p-iNCs were observed by immunocytochemistry. By the expression of DsRed, we confirmed that Tuj1 and MAP2 positive cells were from MEFs but not astrocytes (Figure 7.7 B). From the results, protein-induced neuronal cells (p-iNCs) were led by 30ANR protein.

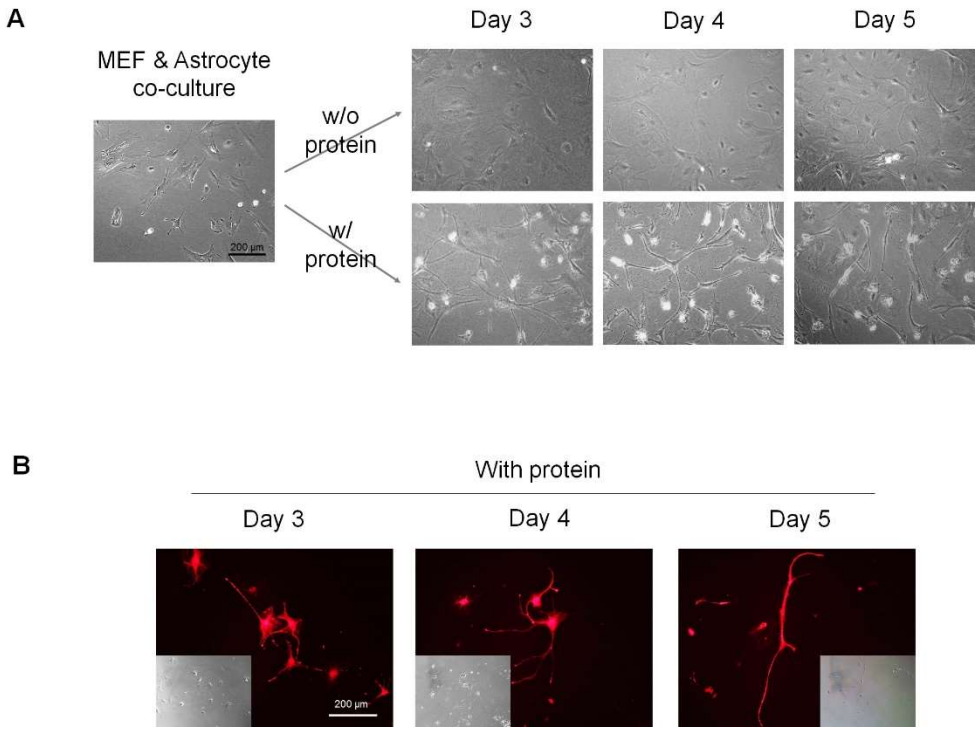

Figure 7.6 Cell morphology change during p-iNCs generation

A. Co-culture of MEFs with astrocytes at day 0. 30ANR protein was added in the cells. B. Fluorescence image for co-culture dish. Neuronal morphology was observed in DsRed MEFs. Scale bar, 200 μm.

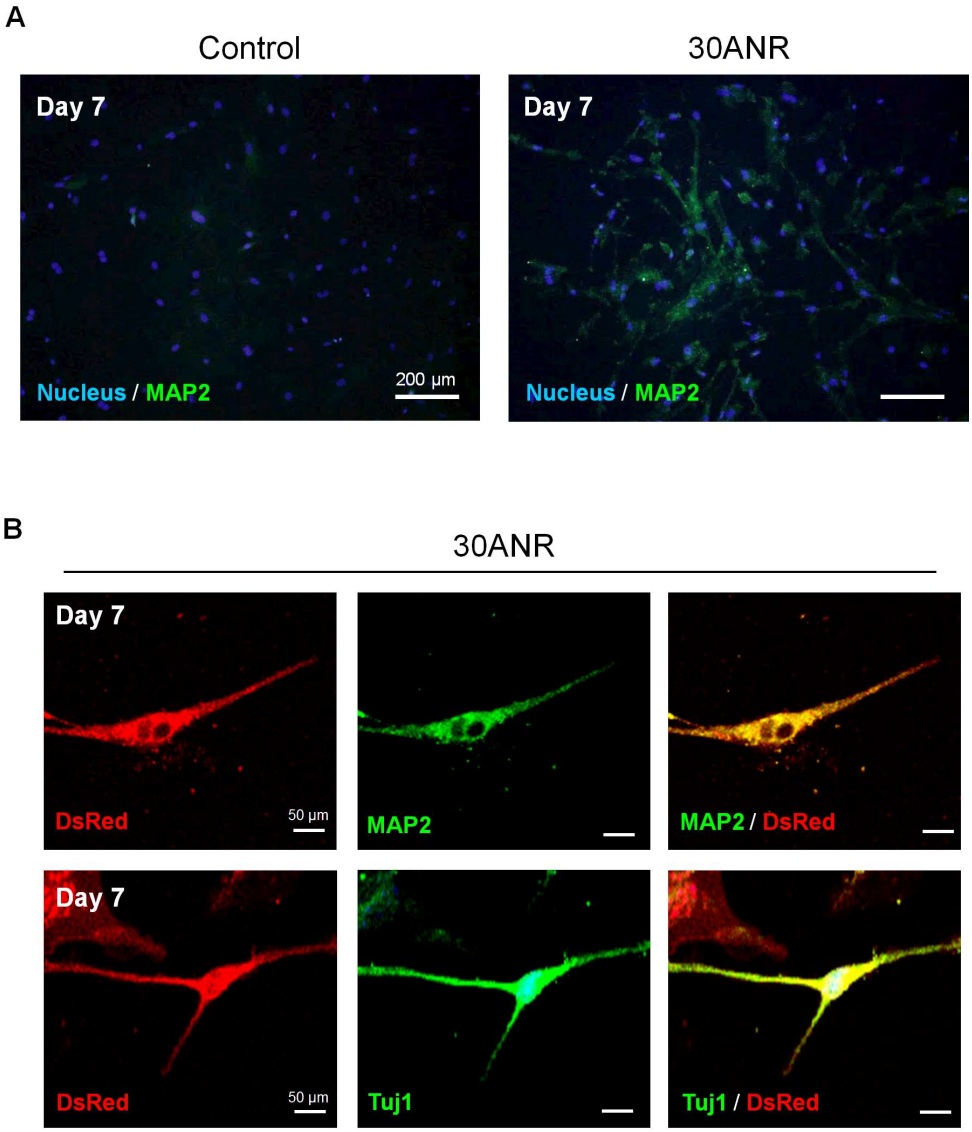

Figure 7.7 Neuronal markers expression in p-iNCs

A. MAP2 expression of p-iNCs at day 7. Scale bar, 200 μm. **B.** MAP2 and Tuj1 neuronal markers were expressed in p-iNCs at day 7. DsRed indicated that the cells were from MEFs. Scale bar is 50 μm.

7.9 Neuronal gene expression in p-iNCs

In order to test in more detail, we measured the endogenous gene levels of *ASCL1*, *BRN2* and *MYT1L* in transitioning MEFs 7 or 14 days after addition of 30ANR reprogramming protein (Figure 7.8). From the data of quantitative RT-qPCR, we found enhancement levels of *ASCL1, BRN2* and *MYT1L* in the reprogramming protein-added cells when compared to the controls. The expression levels of *ASCL1* were increased 7.3 times in p-iNCs at day 7, and 13.1 times at day 14. In the case of *Brn2*, the expression levels were 10.7 or 23.2 times higher in p-iNCs than control cells. The expression level of *Myt1l* at day 7 was 4.9 times, and 6.9 times higher than control cells at day 14. Therefore, p-iNCs showed higher neuronal gene expression than non-protein control cells.

7.10 Electrophysiological recordings

p-iNCs were then further characterized by electrophysiological recordings using whole cell patch-clamp analysis [91]. The neuron-like cell was showed fast-inactivating inward and outward currents (Figure 7.9 A). Also, action potential was observed in cell (Figure 7.9 B). These findings indicate that 30ANR protein could generate

neuronal cells. However, there was relatively small differences between control cells and p-iNCs. Further study could be carried out to generate fully functional p-iNCs.

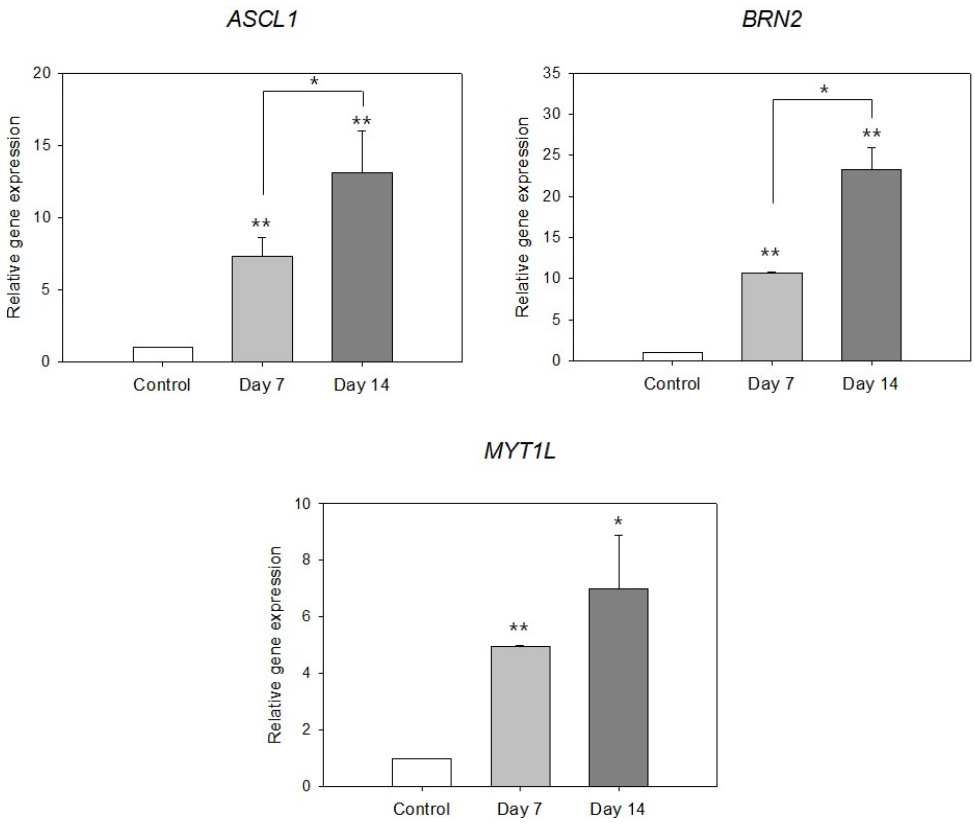

Figure 7.8 Expression of neuronal transcription factors in p-iNCs

ASCL1, *BRN2* and *MYT1L* neuronal gene levels were quantified by RT-qPCR. $*p < 0.05$, $**p < 0.01$ compared with the control group (n = 3). Error bars represent standard deviation.

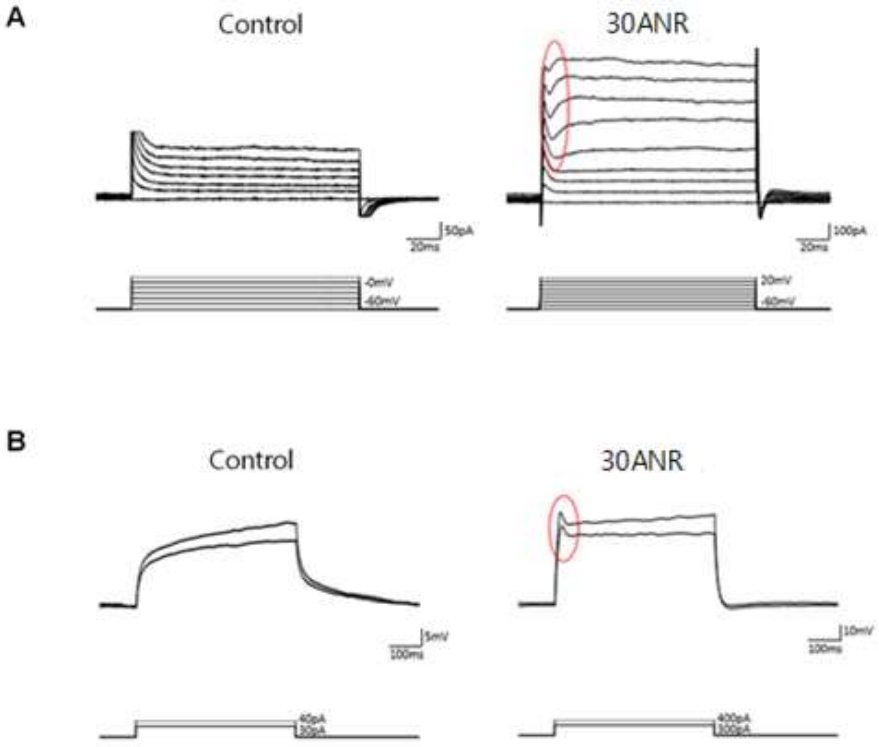

Figure 7.9 Electrophysiological recordings

A. Whole-cell patch clamp recording of p-iNC. B. Action potential.

7.11 Conclusions

In this study, 30Kc19 protein was applied as a fusion partner for soluble expression of a single reprogramming factor Ascl1 and was used for protein-based direct conversion of MEFs to induced neuronal cells (iNCs). We have previously observed that 30Kc19 protein has the potential to be utilized as a fusion partner in the protein-based delivery of reprogramming factors for the regulation of gene expression [73]. Conjugating a cargo to the C-terminus of the 30Kc19 protein enhanced the soluble expression of Yamanaka factors (Oct4, Sox2, c-Myc, Klf4), as well as Ascl1 in our study, while R9 alone did not. This demonstrates that 30Kc19 protein is a promising candidate for soluble expression of reprogramming factors.

With 30ANR protein, we generated p-iNCs successfully. p-iNCs had neuronal morphologies, and expressed neuronal markers, Tuj1 and MAP2. Furthermore, from RT-qPCR data, p-iNCs expressed neuronal gene such as *ASCL1*, *BRN2*, and *MYT1L*. However, small increase in the sodium currents and action potentials demonstrated that 1 master factor-based p-iNCs may not be sufficient to generate a fully functional neuronal cells. It may be that longer period is necessary for the p-iNCs to be fully matured and have functional

electrophysiological properties. This protein method is anticipated to provide a safer generation of patient-specific human neurons for future applications in regenerative medicine.

Chapter 8.

Overall discussion

and further suggestions

Chapter 8. Overall discussion and further suggestions

Our group previously isolated 30Kc6 and 30Kc19 protein from silkworm hemolymph (SH), and have found the properties. 30Kc6 inhibited apoptosis in many type of cells [9, 11]. We assume that 30Kc6 prevents Bax to bind mitochondria [12]. As a result, by preventing to release cytochrome c, cellular apoptosis was inhibited. That is related to apoptosis of intrinsic mitochondrial pathway [92].

Human pluripotent stem cells such as hESC and hiPSC have been induce a rapid apoptosis after apoptotic stimuli [93, 94]. In hESCs, unlike other mammalian cells, pre-activated Bax is existed at the Golgi. When the cells receive apoptotic stimuli, pre-activated Bax rapidly translocated to the mitochondria. Generally, pluripotent stem cells were required mechanical transfer due to preventing for apoptosis, and it was labor intensive and time-consuming [95, 96]. In dissociated pluripotent stem cells, myosin hyper-activation was occurred, and contraction-induced apoptosis is induced by activating caspase through mitochondria [97]. To use up-scaling and handle easy for human pluripotent stem cells, the study of facilitated expansion by enzymatic passaging methods has started in many groups [96, 98-102]. However, inhibition of rapid apoptosis is still a

big hurdle to overcome. In this study, we applied 30Kc6 anti-apoptotic gene in hiPSCs, and observed hiPSC-30Kc6 had higher viability in single-cell enzymatic dissociation. Clear mechanism has to be further studied, but binding of 30Kc6 with Bax might prevent apoptosis in hiPSCs in a similar way in other mammalian cells. Furthermore, due to maintain of Bax at Golgi in hiPSCs, 30Kc6 is considered effective material to inhibit apoptosis specially in hiPSC or hESC.

In apoptosis study, Bcl-2 family are well known as anti-apoptotic proteins by prevention for releasing of cytochrome c from mitochondria [103-105]. To be specific, BH4 domain which is an alpha-helix in Bcl-2 had a role for blocking apoptosis by interacting with Bax [106, 107]. There was a report about BHRF1 derived from Epstein-Barr virus, BHRF1 inhibited apoptosis using structural basis [108]. The structure of BHRF1 is alpha-helix as like BH4 domain, and it inhibited apoptosis by binding pro-apoptotic protein (Bid, Puma, or Bak). From these studies, we hypothesized that 30Kc6α which has structural similarity with other anti-apoptotic proteins, could play a role of apoptosis inhibition in 30Kc6. To observe anti-apoptotic property, we truncated 30Kc6 to 30Kc6α and 30Kc6β,

then tested anti-apoptotic property of 30Kc6α. From the results, 30Kc6α showed similar or higher anti-apoptotic effect than whole 30Kc6. However, the effect was not regular in every cells due to different transfection efficiency. Thus, we tried to produce 30Kc6α as proteins, and 30Kc19 protein was conjugated for enhancement soluble expression and cell-penetration. 30Kc19-30Kc6α protein might be used in biotechnological industry to make valuable products.

30Kc19 protein, one of the 30K members, was applied as a fusion partner for the production of recombinant transcription factors that are used for the generation of iPSCs. Even though the recombinant proteins were produced as soluble forms, the extracellular and intracellular instabilities of these proteins after treatment are a critical problem still requiring a solution. It was reported that unstable soluble proteins are aggregated easily during cell culture [80]. There were trials to increase the stability of proteins by adding supplements such as lipid-rich albumin or serum [109, 110]. We observed that 30Kc19-conjugated transcription factors showed enhanced stability without additive materials to a culture medium. Previously, we reported that 30Kc19 protein increased enzyme stability via shielding effect; possibly by hydrophobic interaction [19]. The increased

stability of transcription factor is also considered to be due to the shielding effect of 30Kc19 protein. From luciferase and immunofluorescence assay, the results indicate that 30Kc19-conjugated with transcription factors enhances the intracellular stability of the protein and thus provides more opportunities for the transcription factor to further penetrate into the nucleus to carry out its role in binding to target DNA to participate in transcription. To accomplish successful protein-based reprogramming, a significant amount of proteins is required [84]. However, because of a cytotoxicity hurdle, a small number of proteins (0.5-8 μg/ml) had to be added repeatedly, and 36 h was required between the cycles [61]. In the case of the 30Kc19-conjugated protein, even when the concentration of total proteins was 60 μg/ml, statistical differences in cytotoxicity were not observed. This demonstrates that 30Kc19 protein is a nontoxic carrier for the delivery of transcription factors and enhances that stability of adjacent proteins. For reprogramming, optimal concentration of proteins has to be tested by considering with toxicity.

Also, we used protein-based approach for generation of induced-neuronal cells (p-iNCs) from co-culture of MEFs and glial

(astrocyte) cells [90]. Recent work has shown that mouse and human fibroblasts (MEFs, HFFs) and embryonic stem cells (mESCs, hESCs) can be directly reprogrammed into mature induced neuronal cells (iNCs) by forced expression of a single reprogramming factor Ascl1, and that Ascl1 is the key driver of iNC reprogramming [29, 111]. However, all methods to generate iNC require the use of genetic materials and/or potentially mutagenic molecules which could potentially be tumorigenic via integration of genetic material into the host cell genome [37, 75]. This protein-based approach is more practical and suitable method for clinical use due to low risks associated with tumorigenicity and genomic integration from the use of genetic materials such as DNA transfection and viruses. In this study, Ascl1 was conjugated with 30Kc19 protein. 30Kc19-Ascl1 protein was enhanced soluble expression in *E. coli*. Also, 30Kc19 protein could drag Ascl1 into cells, and induced neuronal cells. Further study could be carried out to analyze physical property of p-iNCs. Also, investigation whether p-iNCs can be derived from human cells is required. This method is anticipated to provide a safer generation of patient-specific human neurons for future applications in regenerative medicine.

In the thesis, 30Kc6 anti-apoptotic protein and 30Kc19 cell-penetrating protein were applied in cellular reprogramming. These new approaches could be a solution for the technical bottlenecks in stem cell.

Bibliography

[1] Ha, S. H., Park, T. H., and Kim, S.-E., Silkworm hemolymph as a substitute for fetal bovine serum in insect cell culture. *Biotechnology Techniques*, 1996. **10**(6): 401-406.

[2] Ha, S. H. and Park, T. H., Efficient production of recombinant protein in Spodoptera frugiperda/AcNPV system utilizing silkworm hemolymph. *Biotechnology Letters*, 1997. **19**(11): 1087-1091.

[3] Rhee, W. J. and Park, T. H., Silkworm Hemolymph Inhibits Baculovirus-Induced Insect Cell Apoptosis. *Biochemical and Biophysical Research Communications*, 2000. **271**(1): 186-190.

[4] Rhee, W. J., Kim, E. J., and Park, T. H., Kinetic effect of silkworm hemolymph on the delayed host cell death in an insect cell-baculovirus system. *Biotechnol Prog*, 1999. **15**(6): 1028-1032.

[5] Rhee, W. J., Kim, E. J., and Park, T. H., Silkworm hemolymph as a potent inhibitor of apoptosis in Sf9 cells. *Biochem Biophys Res Commun*, 2002. **295**(4): 779-783.

[6] Choi, S. S., Rhee, W. J., and Park, T. H., Inhibition of human cell apoptosis by silkworm hemolymph. *Biotechnol Prog*, 2002. **18**(4): 874-878.

[7] Kim, E. J., Rhee, W. J., and Park, T. H., Isolation and characterization of an apoptosis-inhibiting component from the hemolymph of Bombyx mori. *Biochem Biophys Res Commun*, 2001. **285**(2): 224-228.

[8] Kim, E. J. and Park, T. H., Anti-apoptosis engineering. *Biotechnology and Bioprocess Engineering*, 2003. **8**(2): 76-82.

[9] Kim, E. J., Rhee, W. J., and Park, T. H., Inhibition of apoptosis by a Bombyx mori gene. *Biotechnol Prog*, 2004. **20**(1): 324-329.

[10] Kim, E. J., Park, H. J., and Park, T. H., Inhibition of apoptosis by recombinant 30K protein originating from silkworm hemolymph. *Biochem Biophys Res Commun*, 2003. **308**(3): 523-528.

[11] Park, H. J., Kim, E. J., Koo, T. Y., *et al.*, Purification of recombinant 30K protein produced in Escherichia coli and its anti-apoptotic effect in mammalian and insect cell systems. *Enzyme and Microbial Technology*, 2003. **33**(4): 466-471.

[12] Wang, Z., Ma, X., Fan, L., *et al.*, Understanding the mechanistic roles of 30Kc6 gene in apoptosis and specific productivity in antibody-producing Chinese hamster ovary cells. *Appl Microbiol Biotechnol*, 2012. **94**(5): 1243-1253.

[13] Koo, T. Y., Park, J. H., Park, H. H., *et al.*, Beneficial effect of 30Kc6 gene expression on production of recombinant interferon-β in serum-free suspension culture of CHO cells. *Process Biochemistry*, 2009. **44**(2): 146-153.

[14] Choi, S. S., Rhee, W. J., Kim, E. J., *et al.*, Enhancement of recombinant protein production in Chinese hamster ovary cells through anti-apoptosis engineering using 30Kc6 gene. *Biotechnol Bioeng*, 2006. **95**(3): 459-467.

[15] Park, H. H., Choi, J., Lee, H. J., *et al.*, Enhancement of human erythropoietin production in Chinese hamster ovary cells through supplementation of 30Kc19-30Kc6 fusion protein. *Process Biochemistry*, 2015. **50**(6): 973-980.

[16] Park, J. H., Lee, J. H., Park, H. H., *et al.*, A protein delivery system using 30Kc19 cell-penetrating protein originating from silkworm. *Biomaterials*, 2012. **33**(35): 9127-9134.

[17] Park, H. H., Sohn, Y., Yeo, J. W., *et al.*, Dimerization of 30Kc19

protein in the presence of amphiphilic moiety and importance of Cys-57 during cell penetration. *Biotechnology Journal*, 2014. **9**(12): 1582-1593.

[18] Park, H. H., Sohn, Y., Yeo, J. W., *et al.*, Identification and characterization of a novel cell-penetrating peptide of 30Kc19 protein derived from Bombyx mori. *Process Biochemistry*, 2014. **49**(9): 1516-1526.

[19] Park, J. H., Park, H. H., Choi, S. S., *et al.*, Stabilization of enzymes by the recombinant 30Kc19 protein. *Process Biochemistry*, 2012. **47**(1): 164-169.

[20] Park, J. H., Lee, H. J., Park, H. H., *et al.*, Stabilization of cellular mitochondrial enzyme complex and sialyltransferase activity through supplementation of 30Kc19 protein. *Appl Microbiol Biotechnol*, 2015. **99**(5): 2155-2163.

[21] Lee, H. J., Park, H. H., Kim, J. A., *et al.*, Enzyme delivery using the 30Kc19 protein and human serum albumin nanoparticles. *Biomaterials*, 2014. **35**(5): 1696-1704.

[22] Ryu, J., Kim, H., Park, H. H., *et al.*, Protein-stabilizing and cell-penetrating properties of alpha-helix domain of 30Kc19 protein. *Biotechnol J*, 2016. **11**(11): 1443-1451.

[23] Takahashi, K. and Yamanaka, S., Induction of Pluripotent Stem Cells from Mouse Embryonic and Adult Fibroblast Cultures by Defined Factors. *Cell*, 2006. **126**(4): 663-676.

[24] Takahashi, K., Tanabe, K., Ohnuki, M., *et al.*, Induction of Pluripotent Stem Cells from Adult Human Fibroblasts by Defined Factors. *Cell*, 2007. **131**(5): 861-872.

[25] Choi, J., Costa, M. L., Mermelstein, C. S., *et al.*, MyoD converts primary dermal fibroblasts, chondroblasts, smooth muscle, and retinal pigmented epithelial cells into striated mononucleated myoblasts and multinucleated myotubes. *Proc Natl Acad Sci U S A*, 1990. **87**(20): 7988-7992.

[26] Ieda, M., Fu, J. D., Delgado-Olguin, P., *et al.*, Direct reprogramming of fibroblasts into functional cardiomyocytes by defined factors. *Cell*, 2010. **142**(3): 375-386.

[27] Zhou, Q., Brown, J., Kanarek, A., *et al.*, In vivo reprogramming of adult pancreatic exocrine cells to [bgr]-cells. *Nature*, 2008. **455**(7213): 627-632.

[28] Ginsberg, M., James, D., Ding, B. S., *et al.*, Efficient direct reprogramming of mature amniotic cells into endothelial cells by ETS factors and TGFbeta suppression. *Cell*, 2012. **151**(3): 559-575.

[29] Vierbuchen, T., Ostermeier, A., Pang, Z. P., *et al.*, Direct conversion of fibroblasts to functional neurons by defined factors. *Nature*, 2010. **463**(7284): 1035-1041.

[30] Yamada, S., Yamamoto, Y., Nagasawa, M., *et al.*, In vitro transdifferentiation of mature hepatocytes into insulin-producing cells. *Endocr J*, 2006. **53**(6): 789-795.

[31] Lowry, W. E., Richter, L., Yachechko, R., *et al.*, Generation of human induced pluripotent stem cells from dermal fibroblasts. *Proc Natl Acad Sci U S A*, 2008. **105**(8): 2883-2888.

[32] Huangfu, D., Osafune, K., Maehr, R., *et al.*, Induction of pluripotent stem cells from primary human fibroblasts with only Oct4 and Sox2. *Nat Biotech*, 2008. **26**(11): 1269-1275.

[33] Aasen, T., Raya, A., Barrero, M. J., *et al.*, Efficient and rapid generation of induced pluripotent stem cells from human keratinocytes. *Nat Biotechnol*, 2008. **26**(11): 1276-1284.

[34] Yu, J., Vodyanik, M. A., Smuga-Otto, K., *et al.*, Induced pluripotent stem cell lines derived from human somatic cells. *Science*, 2007. **318**(5858): 1917-1920.

[35] Stadtfeld, M., Brennand, K., and Hochedlinger, K., Reprogramming of pancreatic beta cells into induced

pluripotent stem cells. *Curr Biol*, 2008. **18**(12): 890-894.

[36] Sommer, C. A., Stadtfeld, M., Murphy, G. J., *et al.*, Induced pluripotent stem cell generation using a single lentiviral stem cell cassette. *Stem Cells*, 2009. **27**(3): 543-549.

[37] Maherali, N., Ahfeldt, T., Rigamonti, A., *et al.*, A high-efficiency system for the generation and study of human induced pluripotent stem cells. *Cell Stem Cell*, 2008. **3**(3): 340-345.

[38] Stadtfeld, M., Maherali, N., Breault, D. T., *et al.*, Defining molecular cornerstones during fibroblast to iPSC reprogramming in mouse. *Cell Stem Cell*, 2008. **2**(3): 230-240.

[39] Stadtfeld, M., Nagaya, M., Utikal, J., *et al.*, Induced pluripotent stem cells generated without viral integration. *Science*, 2008. **322**(5903): 945-949.

[40] Zhou, W. and Freed, C. R., Adenoviral gene delivery can reprogram human fibroblasts to induced pluripotent stem cells. *Stem Cells*, 2009. **27**(11): 2667-2674.

[41] Fusaki, N., Ban, H., Nishiyama, A., *et al.*, Efficient induction of transgene-free human pluripotent stem cells using a vector based on Sendai virus, an RNA virus that does not integrate into the host genome. *Proc Jpn Acad Ser B Phys Biol Sci*, 2009. **85**(8): 348-362.

[42] Ban, H., Nishishita, N., Fusaki, N., *et al.*, Efficient generation of transgene-free human induced pluripotent stem cells (iPSCs) by temperature-sensitive Sendai virus vectors. *Proc Natl Acad Sci U S A*, 2011. **108**(34): 14234-14239.

[43] Seki, T., Yuasa, S., Oda, M., *et al.*, Generation of Induced Pluripotent Stem Cells from Human Terminally Differentiated Circulating T Cells. *Cell Stem Cell*, 2010. **7**(1): 11-14.

[44] Okita, K., Nakagawa, M., Hyenjong, H., *et al.*, Generation of mouse induced pluripotent stem cells without viral vectors. *Science*, 2008. **322**(5903): 949-953.

[45] Si-Tayeb, K., Noto, F. K., Sepac, A., *et al.*, Generation of human induced pluripotent stem cells by simple transient transfection of plasmid DNA encoding reprogramming factors. *BMC Dev Biol*, 2010. **10**: 81.

[46] Chen, Z. Y., He, C. Y., Ehrhardt, A., *et al.*, Minicircle DNA vectors devoid of bacterial DNA result in persistent and high-level transgene expression in vivo. *Mol Ther*, 2003. **8**(3): 495-500.

[47] Chen, Z. Y., He, C. Y., and Kay, M. A., Improved production and purification of minicircle DNA vector free of plasmid bacterial sequences and capable of persistent transgene expression in vivo. *Hum Gene Ther*, 2005. **16**(1): 126-131.

[48] Jia, F., Wilson, K. D., Sun, N., *et al.*, A nonviral minicircle vector for deriving human iPSCs. *Nat Methods*, 2010. **7**(3): 197-199.

[49] Cheng, L., Hansen, N. F., Zhao, L., *et al.*, Low incidence of DNA sequence variation in human induced pluripotent stem cells generated by nonintegrating plasmid expression. *Cell Stem Cell*, 2012. **10**(3): 337-344.

[50] Narsinh, K. H., Jia, F., Robbins, R. C., *et al.*, Generation of adult human induced pluripotent stem cells using nonviral minicircle DNA vectors. *Nat Protoc*, 2011. **6**(1): 78-88.

[51] Warren, L., Manos, P. D., Ahfeldt, T., *et al.*, Highly efficient reprogramming to pluripotency and directed differentiation of human cells with synthetic modified mRNA. *Cell Stem Cell*, 2010. **7**(5): 618-630.

[52] Miyoshi, N., Ishii, H., Nagano, H., *et al.*, Reprogramming of mouse and human cells to pluripotency using mature

microRNAs. *Cell Stem Cell*, 2011. **8**(6): 633-638.

[53] Subramanyam, D., Lamouille, S., Judson, R. L.*, et al.*, Multiple targets of miR-302 and miR-372 promote reprogramming of human fibroblasts to induced pluripotent stem cells. *Nat Biotechnol*, 2011. **29**(5): 443-448.

[54] Anokye-Danso, F., Trivedi, C. M., Juhr, D.*, et al.*, Highly efficient miRNA-mediated reprogramming of mouse and human somatic cells to pluripotency. *Cell Stem Cell*, 2011. **8**(4): 376-388.

[55] Soldner, F., Hockemeyer, D., Beard, C.*, et al.*, Parkinson's disease patient-derived induced pluripotent stem cells free of viral reprogramming factors. *Cell*, 2009. **136**(5): 964-977.

[56] Chakraborty, S., Christoforou, N., Fattahi, A.*, et al.*, A Robust Strategy for Negative Selection of Cre-LoxP Recombination-Based Excision of Transgenes in Induced Pluripotent Stem Cells. *PLoS ONE*, 2013. **8**(5): e64342.

[57] Kaji, K., Norrby, K., Paca, A.*, et al.*, Virus-free induction of pluripotency and subsequent excision of reprogramming factors. *Nature*, 2009. **458**(7239): 771-775.

[58] Mali, P., Chou, B. K., Yen, J.*, et al.*, Butyrate greatly enhances derivation of human induced pluripotent stem cells by promoting epigenetic remodeling and the expression of pluripotency-associated genes. *Stem Cells*, 2010. **28**(4): 713-720.

[59] Ivics, Z., Izsvak, Z., Medrano, G.*, et al.*, Sleeping Beauty transposon mutagenesis in rat spermatogonial stem cells. *Nat. Protocols*, 2011. **6**(10): 1521-1535.

[60] Kim, D., Kim, C. H., Moon, J. I.*, et al.*, Generation of human induced pluripotent stem cells by direct delivery of reprogramming proteins. *Cell Stem Cell*, 2009. **4**(6): 472-476.

[61] Zhou, H., Wu, S., Joo, J. Y., *et al.*, Generation of Induced Pluripotent Stem Cells Using Recombinant Proteins. *Cell Stem Cell*, 2009. **4**(5): 381-384.

[62] Desai, N., Rambhia, P., and Gishto, A., Human embryonic stem cell cultivation: historical perspective and evolution of xeno-free culture systems. *Reproductive Biology and Endocrinology : RB&E*, 2015. **13**: 9.

[63] Turner, W. S. and McCloskey, K. E., Rapid Fibroblast Removal from High Density Human Embryonic Stem Cell Cultures. *Journal of Visualized Experiments : JoVE*, 2012(68): 3951.

[64] Joza, N., Susin, S. A., Daugas, E., *et al.*, Essential role of the mitochondrial apoptosis-inducing factor in programmed cell death. *Nature*, 2001. **410**(6828): 549-554.

[65] Hong, H., Takahashi, K., Ichisaka, T., *et al.*, Suppression of induced pluripotent stem cell generation by the p53-p21 pathway. *Nature*, 2009. **460**(7259): 1132-1135.

[66] Guo, Y., Mantel, C., Hromas, R. A., *et al.*, Oct-4 is critical for survival/antiapoptosis of murine embryonic stem cells subjected to stress: effects associated with Stat3/survivin. *Stem Cells*, 2008. **26**(1): 30-34.

[67] Hockemeyer, D., Wang, H., Kiani, S., *et al.*, Genetic engineering of human pluripotent cells using TALE nucleases. *Nat Biotechnol*, 2011. **29**(8): 731-734.

[68] Wang, Z., Ma, X., Zhao, L., *et al.*, Expression of anti-apoptotic 30Kc6 gene inhibiting hyperosmotic pressure-induced apoptosis in antibody-producing Chinese hamster ovary cells. *Process Biochemistry*, 2012. **47**(5): 735-741.

[69] Shimohama, S., Apoptosis in Alzheimer's disease--an update. *Apoptosis*, 2000. **5**(1): 9-16.

[70] Dickson, D. W., Apoptotic mechanisms in Alzheimer

neurofibrillary degeneration: cause or effect? *Journal of Clinical Investigation*, 2004. **114**(1): 23-27.

[71] Janumyan, Y. M., Sansam, C. G., Chattopadhyay, A.*, et al.*, Bcl-xL/Bcl-2 coordinately regulates apoptosis, cell cycle arrest and cell cycle entry. *Embo j*, 2003. **22**(20): 5459-5470.

[72] Oudejans, J. J., van den Brule, A. J., Jiwa, N. M.*, et al.*, BHRF1, the Epstein-Barr virus (EBV) homologue of the BCL-2 protooncogene, is transcribed in EBV-associated B-cell lymphomas and in reactive lymphocytes. *Blood*, 1995. **86**(5): 1893-1902.

[73] Ryu, J., Park, H. H., Park, J. H.*, et al.*, Soluble expression and stability enhancement of transcription factors using 30Kc19 cell-penetrating protein. *Appl Microbiol Biotechnol*, 2016. **100**(8): 3523-3532.

[74] Boulikas, T., Putative nuclear localization signals (NLS) in protein transcription factors. *J Cell Biochem*, 1994. **55**(1): 32-58.

[75] Maherali, N. and Hochedlinger, K., Guidelines and techniques for the generation of induced pluripotent stem cells. *Cell Stem Cell*, 2008. **3**(6): 595-605.

[76] Chou, B. K., Mali, P., Huang, X.*, et al.*, Efficient human iPSC derivation by a non-integrating plasmid from blood cells with unique epigenetic and gene expression signatures. *Cell Res*, 2011. **21**(3): 518-529.

[77] Woltjen, K., Michael, I. P., Mohseni, P.*, et al.*, piggyBac transposition reprograms fibroblasts to induced pluripotent stem cells. *Nature*, 2009. **458**(7239): 766-770.

[78] Hou, Z., Zhang, Y., Propson, N. E.*, et al.*, Efficient genome engineering in human pluripotent stem cells using Cas9 from Neisseria meningitidis. *Proceedings of the National Academy of Sciences*, 2013. **110**(39): 15644-15649.

[79] Mossakowska, D. E., Expression of nuclear hormone receptors in Escherichia coli. *Curr Opin Biotechnol*, 1998. **9**(5): 502-505.

[80] Sorensen, H. P. and Mortensen, K. K., Soluble expression of recombinant proteins in the cytoplasm of Escherichia coli. *Microb Cell Fact*, 2005. **4**(1): 1.

[81] Chan, P., Curtis, R. A., and Warwicker, J., Soluble expression of proteins correlates with a lack of positively-charged surface. *Scientific Reports*, 2013. **3**: 3333.

[82] Chang, C. C., Song, J., Tey, B. T.*, et al.*, Bioinformatics approaches for improved recombinant protein production in Escherichia coli: protein solubility prediction. *Brief Bioinform*, 2014. **15**(6): 953-962.

[83] Smialowski, P., Martin-Galiano, A. J., Mikolajka, A.*, et al.*, Protein solubility: sequence based prediction and experimental verification. *Bioinformatics*, 2007. **23**(19): 2536-2542.

[84] Yang, W. C., Patel, K. G., Lee, J.*, et al.*, Cell-free production of transducible transcription factors for nuclear reprogramming. *Biotechnol Bioeng*, 2009. **104**(6): 1047-1058.

[85] Golovanov, A. P., Hautbergue, G. M., Wilson, S. A.*, et al.*, A simple method for improving protein solubility and long-term stability. *J Am Chem Soc*, 2004. **126**(29): 8933-8939.

[86] Hu, P. F., Guan, W. J., Li, X. C.*, et al.*, Construction of recombinant proteins for reprogramming of endangered Luxi cattle fibroblast cells. *Mol Biol Rep*, 2012. **39**(6): 7175-7182.

[87] Pan, C., Lu, B., Chen, H.*, et al.*, Reprogramming human fibroblasts using HIV-1 TAT recombinant proteins OCT4, SOX2, KLF4 and c-MYC. *Mol Biol Rep*, 2010. **37**(4): 2117-2124.

[88] Nakagawa, M., Koyanagi, M., Tanabe, K.*, et al.*, Generation of

induced pluripotent stem cells without Myc from mouse and human fibroblasts. *Nat Biotechnol*, 2008. **26**(1): 101-106.

[89] Nakagawa, M., Takizawa, N., Narita, M., *et al.*, Promotion of direct reprogramming by transformation-deficient Myc. *Proc Natl Acad Sci U S A*, 2010. **107**(32): 14152-14157.

[90] Chanda, S., Ang, C. E., Davila, J., *et al.*, Generation of induced neuronal cells by the single reprogramming factor ASCL1. *Stem Cell Reports*, 2014. **3**(2): 282-296.

[91] Halder, D., Lee, C., Hyun, J. Y., et al., Supression of Sin3A activity promotes differentiation of pluripotent cells into functional neurons. *Scientific reports*, 2017. **7**:44818.

[92] Elmore, S., Apoptosis: A Review of Programmed Cell Death. *Toxicologic pathology*, 2007. **35**(4): 495-516.

[93] Dumitru, R., Gama, V., Fagan, B. M., *et al.*, Human Embryonic Stem Cells have Constitutively Active Bax at the Golgi and are Primed to Undergo Rapid Apoptosis. *Mol Cell*, 2012. **46**(5): 573-583.

[94] Nichols, J. and Smith, A., Naive and Primed Pluripotent States. *Cell Stem Cell*, 2009. **4**(6): 487-492.

[95] Hou, Z., Zhang, Y., Propson, N. E., *et al.*, Efficient genome engineering in human pluripotent stem cells using Cas9 from Neisseria meningitidis. *Proc Natl Acad Sci U S A*, 2013. **110**(39): 15644-15649.

[96] Oh, S. K., Kim, H. S., Park, Y. B., *et al.*, Methods for expansion of human embryonic stem cells. *Stem Cells*, 2005. **23**(5): 605-609.

[97] Ohgushi, M. and Sasai, Y., Lonely death dance of human pluripotent stem cells: ROCKing between metastable cell states. *Trends Cell Biol*, 2011. **21**(5): 274-282.

[98] Sjogren-Jansson, E., Zetterstrom, M., Moya, K., *et al.*, Large-scale propagation of four undifferentiated human embryonic stem cell lines in a feeder-free culture system. *Dev Dyn*, 2005. **233**(4): 1304-1314.

[99] Carpenter, M. K., Rosler, E. S., Fisk, G. J., *et al.*, Properties of four human embryonic stem cell lines maintained in a feeder-free culture system. *Dev Dyn*, 2004. **229**(2): 243-258.

[100] Cowan, C. A., Klimanskaya, I., McMahon, J., *et al.*, Derivation of embryonic stem-cell lines from human blastocysts. *N Engl J Med*, 2004. **350**(13): 1353-1356.

[101] Choo, A. B., Padmanabhan, J., Chin, A. C., *et al.*, Expansion of pluripotent human embryonic stem cells on human feeders. *Biotechnol Bioeng*, 2004. **88**(3): 321-331.

[102] Ellerstrom, C., Strehl, R., Noaksson, K., *et al.*, Facilitated expansion of human embryonic stem cells by single-cell enzymatic dissociation. *Stem Cells*, 2007. **25**(7): 1690-1696.

[103] Yang, J., Liu, X., Bhalla, K., *et al.*, Prevention of apoptosis by Bcl-2: release of cytochrome c from mitochondria blocked. *Science*, 1997. **275**(5303): 1129-1132.

[104] Czabotar, P. E., Lessene, G., Strasser, A., *et al.*, Control of apoptosis by the BCL-2 protein family: implications for physiology and therapy. *Nat Rev Mol Cell Biol*, 2014. **15**(1): 49-63.

[105] Tsujimoto, Y., Role of Bcl-2 family proteins in apoptosis: apoptosomes or mitochondria? *GenESCs*, 1998. **3**(11): 697-707.

[106] Barclay, L. A., Wales, T. E., Garner, T. P., *et al.*, Inhibition of Pro-apoptotic BAX by a noncanonical interaction mechanism. *Mol Cell*, 2015. **57**(5): 873-886.

[107] Willis, S., Day, C. L., Hinds, M. G., *et al.*, The Bcl-2-regulated

apoptotic pathway. *Journal of Cell Science*, 2003. **116**(20): 4053.

[108] Kvansakul, M., Wei, A. H., Fletcher, J. I., *et al.*, Structural basis for apoptosis inhibition by Epstein–Barr virus BHRF1. *PLoS Pathog*, 2010. **6**(12): e1001236.

[109] Thier, M., Munst, B., and Edenhofer, F., Exploring refined conditions for reprogramming cells by recombinant Oct4 protein. *Int J Dev Biol*, 2010. **54**(11–12): 1713–1721.

[110] Thier, M., Münst, B., Mielke, S., *et al.*, Cellular reprogramming employing recombinant sox2 protein. *Stem cells international*, 2012. **2012**.

[111] Pang, Z. P., Yang, N., Vierbuchen, T., *et al.*, Induction of human neuronal cells by defined transcription factors. *Nature*, 2011. **476**(7359): 220–223.

국 문 초 록

30Kc6 유전자를 이용한 역분화줄기세포의 세포자멸 억제 효과 및 세포 직접변환을 위한 30Kc19 단백질 기반 전사인자의 효율적인 전달

유 지 나

공과대학 협동과정 바이오엔지니어링

서울대학교 대학원

누에 체액 유래 30K 단백질은 다양한 기능을 가지는 것으로 알려져 있다. 그 중에서도 세포의 생존율을 올리는 것이 맨 처음 알려졌는데, 그 기능은 30K family (30Kc6, 30Kc12, 30Kc19, 30Kc21, 30Kc23) 중 30Kc6가 담당 하는 것으로 알려졌다. 지난연구에서 30Kc6는 이를 세포에 발현 시켰을 때, 세포의 성장을 돕고 세포자멸 (apoptosis) 을 막아주는 기능을 보였다. 이와 같은 결과는 세포에서 항체 및 다양한 단백질 생산 효율을 올리는데 기여할 수 있었다. 30Kc6의 세포자멸 억제

기작은 미토콘드리아에 Bax가 결합하지 못하도록 하는 것인데, 30Kc6를 세포에 발현시킨 후 세포자멸을 유도하였을 때, Bax가 미토콘드리아에 결합하지 못하여 cytochrome c가 나오지 못하는 것을 발견할 수 있었다. 또 다른 30K 단백질 중 하나인 30Kc19 단백질은 세포 투과 펩타이드 (Pep-c19) 를 가지고 있어 세포 안으로 들어가며, 이 때 단백질 이합체를 형성하는 것으로 알려졌다. 30Kc19 단백질은 또한 효소와 같은 단백질의 안정성을 올릴 수 있었는데, 이는 BSA와 같이 주변을 감싸 외부 공격으로부터 단백질을 보호하는 역할을 하는 것으로 고려된다. 또한 최근에는 30Kc19이 결합된 단백질의 수용성 생산을 늘리는 것을 밝혔다.

이 연구의 목적은 30K 단백질의 이러한 특성들을 이용하여, 줄기세포 연구가 가지는 한계를 극복하고자 하는데 있다. 먼저, 배양 과정이 노동집약적이고 단일 세포로 떨어졌을 때 빠른 세포자멸이 일어나는 역분화줄기세포에 30Kc6를 적용하여, 단일세포에서 세포 생존율을 올렸다. 이러한 특징을 보기에 앞서 30Kc6가 들어가도 역분화줄기세포의 다능성에 변화가 없는지를 확인하였고, 세가지 배엽으로 분화가 가능한지를 보았다. 그 결과 30Kc6를 가지는 역분화줄기세포는 줄기세포의 특징은 잃지 않으면서, 단일세포에서 세포자멸이 억제되는 것을 확인하였다.

다음으로 30Kc6의 세포자멸 억제효과가 N-terminal의 30Kc6α에 의한 것이라는 것을 밝혔다. 대표적인 세포자멸 억제 단백질인 Bcl2

의 기작을 보았을 때 알파나선 구조가 Bax 단백질에 결합하여, Bax의 활성을 저해하는 것으로 알려졌다. 이러한 문헌을 토대로 30Kc6의 알파나선 구조 (30Kc6α)가 세포자멸 억제 효과를 낼 것으로 기대하였다. 세포에 30Kc6α를 도입한 결과 해당 세포는 세포자멸 억제 효과가 있는 것으로 보였으며, 이는 30Kc6를 도입한 것보다도 더 좋은 효과였다. 따라서 30Kc6의 세포자멸 억제 효과는 30Kc6α가 담당하는 것으로 결론을 지을 수 있었으며, 30Kc6α를 단백질로 생산하기 위해 세포 투과 30Kc19 단백질을 유전적으로 결합시켜 생산하였다. 그 결과 30K19-30Kc6α 단백질은 수용성 형태로 생산이 되었으며, 세포 투과기능이 있는 것으로 보였다. 또한 재조합 단백질을 세포에 처리하고 세포자멸을 유도하였을 때 단백질을 처리한 농도에 비례하여 세포 생존율이 올라가는 것을 보았다.

세포 투과 단백질인 30Kc19은 세포 리프로그래밍을 위한 전사인자들 (Oct4, Sox2, c-Myc, Klf4, L-Myc) 에 유전적으로 결합되어 생산되었다. 전사인자 단독만으로는 수용성으로 생산되지 않던 Oct4와 L-Myc단백질도 30Kc19이 결합된 후 수용성으로 생산이 되었다. 뿐만 아니라 30Kc19이 결합된 전사인자들은 37℃에서 좀 더 나은 안정성을 보였다. 세포 리프로그래밍에서 단백질의 대량생산과 안정성 문제를 해결하는 것은 매우 큰 과제이기 때문에, 30Kc19 단백질을 이용하여 이 부분에서 효과를 본 것은 매우 큰 의미가 있다. 마지막으로 30Kc19과

결합된 전사인자는 세포의 핵 안으로 들어가 전사 단백질의 활동을 할 수 있음을 보았다.

전사인자가 30Kc19단백질과 결합하여 수용성 생산량이 늘고 세포로 잘 들어가는 것을 확인한 후, 우리는 신경세포를 유도하는 전사인자인 Ascl1을 30Kc19에 결합하여 세포의 직접 변환을 시도하였다. 생산된 30Kc19-Ascl1-NLS-R9 단백질은 세포에 잘 들어가서 전사를 조절하여, 피부세포를 신경세포로 직접변환을 시켰다. 단백질로 유도된 신경세포는 신경세포 유전자와 단백질을 가지는 것으로 확인되었다.

본 연구에서는 30K 단백질 중 세포자멸 억제 단백질인 30Kc6와 세포 투과 단백질인 30Kc19을 이용하여 이를 줄기세포에 적용하였으며, 줄기세포연구가 가지는 여러가지 한계들을 해결할 수 있었다. 앞으로도 이러한 30K 단백질은 줄기세포 뿐 아니라 제약산업, 화장품 산업 등에서 여러가지 공정기술 개발에 유용하게 사용될 수 있을 것으로 기대된다.

주요어: 30K 단백질, 30Kc6, 30Kc19, 세포자멸 억제, 세포 투과, 재조합 단백질, 전사인자, 줄기세포, 세포 리프로그래밍

학 번: 2010-21054